UNIVERSITÀ
DEGLI STUDI
DI PADOVA

Sede Amministrativa: Università degli Studi di Padova

Dipartimento di Istologia, Microbiologia e Biotecnologie Mediche, Sezione di Istologia ed Embriologia

SCUOLA DI DOTTORATO DI RICERCA IN: BIOSCIENZE
INDIRIZZO: GENETICA E BIOLOGIA MOLECOLARE DELLO SVILUPPO
CICLO XXII

Negative control of Smad activity patterns the mammalian embryo

Direttore della Scuola: Ch.mo Prof. Tullio Pozzan
Coordinatore d'indirizzo: Ch.mo Prof. Paolo Bonaldo
Supervisore: Ch.mo Prof. Stefano Piccolo

Dottorando: Leonardo Morsut

INDEX

INDEX 3
ABSTRACT (ENGLISH) 5
ABSTRACT (ITALIAN) 7
PUBLICATIONS 9
INTRODUCTION 11
ANATOMY OF EARLY MOUSE DEVELOPMENT 11
THE TGFβ SIGNALING PATHWAY 13
UBIQUITIN-DEPENDENT REGULATION OF TGFβ SIGNALING 15
MULTIPLE ROLES OF TGFβ LIGANDS DURING EARLY MOUSE DEVELOPMENT 17
RESULTS 24
ECTO HOMOZYGOUS MUTANT EMBRYOS DISPLAY PROFOUND DEFECTS IN POLARITY AND PATTERNING BEFORE GASTRULATION 24
DEFECTIVE AVE PATTERNING IN *ECTO* MUTANTS IS A CELL AUTONOMOUS DEFECT 25
AVE EXPANSION IN *ECTO* MUTANTS IS MEDIATED BY SMAD4 25
AVE DEFECTS IN *ECTO-/-* EMBRYOS ARE DUE TO UNRESTRAINED NODAL SIGNALING 26
ECTO MAINTAINS THE TROPHOBLAST COMPARTMENT BY OPPOSING NODAL SIGNALING 26
ECTO MAINTAINS EXE SELF-RENEWAL 27
ECTO PREVENTS NODAL-INDUCED DIFFERENTIATION OF TROPHOBLAST STEM CELLS 27
LACK OF MESODERM IN *ECTO* MUTANTS IS CAUSED BY EXCESSIVE NODAL AND DEFECTIVE EXE DEVELOPMENT 28
ECTO EXPRESSION IS PATTERNED BEFORE GASTRULATION, ECTO ACTIVITY IS PATTERNED AFTER MESODERM INDUCTION 29
MASSIVE ORGANIZER INDUCTION IN EPIBLAST-SPECIFIC *ECTO* MUTANTS (*EPIKO*) 29
DISCUSSION 32
EXPERIMENTAL PROCEDURES 37
GENOTYPING 37
GENERATION OF *ECTO* KNOCKOUT AND CONDITIONAL ALLELES 37
GENERATION OF *ECTO-EPIKO* AND COMPOUND *ECTO-/-;SMAD4-/-* AND *ECTO-/-;NODALΔ600/-* EMBRYOS 38
IN SITU HYBRIDIZATION 38
IMMUNOFLUORESCENCE AND HISTOLOGY 39
TS CELL CULTURE 40
QPCR ANALYSIS 40
IMMUNOPRECIPITATIONS AND WESTERN BLOTTING 40
REFERENCES 43
FIGURES 48
FIGURE 1. EARLY MOUSE EMBRYONIC DEVELOPMENT. 49
FIGURE 2. THE ORGANIZER/NODE OF THE MOUSE EMBRYO. 51
FIGURE 3. THE TRANSFORMING GROWTH FACTOR-β (TGFβ) SIGNAL TRANSDUCTION PATHWAY. 53
FIGURE 4. MAJOR TGFβ ROLES DURING EARLY MOUSE DEVELOPMENT. 55
FIGURE 5. GENERATION OF *ECTO* ALLELES AND *ECTO-/-* EMBRYOS MORPHOLOGY. 57
FIGURE 6. IMPAIRED MESODERM MASTER GENES INDUCTION IN *ECTO-/-* EMBRYOS. 59
FIGURE 7. *ECTO* HOMOZYGOUS MUTANT EMBRYOS DISPLAY ABNORMALLY EXPANDED ANTERIOR VISCERAL ENDODERM (AVE). 61
FIGURE 9. DEFECTIVE AVE PATTERNING IN *ECTO* MUTANTS IS MEDIATED BY SMAD4. 65
FIGURE 12. *ECTO* PREVENTS NODAL-INDUCED DIFFERENTIATION OF TROPHOBLAST STEM (TS) CELLS. 71

FIGURE 13. *ECTO-/-* EMBRYOS ALLOW EXPLORING THE HIGH SIGNALING PART OF THE FRENCH FLAG FOR NODAL SIGNALING IN EXE. 73
FIGURE 14. LACK OF MESODERM IN *ECTO* MUTANTS IS CAUSED BY EXCESSIVE NODAL AND DEFECTIVE EXE DEVELOPMENT. 75
FIGURE 15. MASSIVE ORGANIZER INDUCTION IN EPIBLAST-SPECIFIC *ECTO* MUTANTS (*EPIKO*). 77
FIGURE 16. EARLY NODAL RELATED DEFECTS IN EPIBLAST SPECIFIC *ECTO* KNOCKOUT EMBRYOS, AND SCHEMES OF THE PROPOSED MODEL. 79
SUPPLEMENTAL TABLE 1 81
SUPPLEMENTAL TABLE 2 83

ACKNOWLEDGMENTS 85

ABSTRACT (ENGLISH)

The definition of embryonic potency and induction of specific cell fates are intimately linked to the tight control over TGFβ signaling. Although extracellular regulation of ligand availability has received considerable attention in recent years, surprisingly little is known on the intracellular factors that negatively control Smad activity in mammalian tissues. By means of genetic ablation, here we show that the Smad4 inhibitor Ectodermin (Ecto, also known as TRIM33 or Tif1γ) is required to allow Nodal morphogenetic properties in early mouse embryo. Loss of Ecto invariably drives Nodal responsiveness to the highest, Smad4-dependent threshold of activity; new phenotypes, linked to excessive Nodal activity, emerge from such a modified landscape of Smad responsiveness in both embryonic and extraembryonic territories. In extraembryonic endoderm, Ecto is required to confine expression of Nodal antagonists to the Anterior Visceral Endoderm. In trophoblast cells, Ecto precisely doses Nodal activity, balancing stem cell self-renewal and differentiation. Epiblast-specific Ecto deficiency shifts mesoderm fates toward Node/Organizer fates, revealing the requirement of Smad4 inhibition for the precise allocation of cells along the primitive streak. This study unveils that intracellular control of Smad function by Ecto/Tif1γ is an integral component of how cells read TGFβ signals.

ABSTRACT (ITALIAN)

La regolazione della pluripotenza e l'induzione di specifici percorsi di differenziamento cellulare sono intimamente connessi a uno stretto controllo della via di segnalazione del TGFβ. La regolazione della parte extracellulare di questa via, cioè quella che concerne la biodisponibilità del ligando, è stata oggetto di numerosi studi in anni recenti. Per quanto riguarda invece la parte intracellulare, pochissimo è noto sull'importanza di fattori che controllino in modo negativo l'attività delle Smad nelle cellule dei tessuti di mammifero. Tramite ablazione genetica, con questo studio dimostriamo come l'inibizione di Smad4 da parte di Ectodermin/Tif1γ/TRIM33 (Ecto) sia richiesta per permettere a Nodal (il ligando TGFβ per eccellenza durante lo sviluppo embrionale mammifero) di svolgere le sue funzioni morfogenetiche durante l'embriogenesi murina. La delezione di Ecto sposta le risposte a Nodal sulla finestra di responsività massima, Smad4 dipendente. In questa situazione di ipereccitata responsività alla segnalazione da parte di Smad, emergono fenotipi nuovi sia in tessuti embrionali che extraembrionali, che sono legati ad un'eccessiva attività di Nodal. Nell'endoderma extraembrionale, Ecto serve per confinare l'espressione degli antagonisti di Nodal nell'endoderma viscerale anteriore. Nelle cellule del trofoblasto, Ecto dosa in modo preciso l'attività di Nodal, permettendo l'instaurarsi del delicato equilibrio tra crescita staminale e differenziamento. La delezione di Ecto specificamente nell'epiblasto incanala il differenziamento del mesoderma verso destini di nodo/tessuto organizzatore, mostrando come sia necessaria un'inibizione di Smad4 per permettere l'allocazione ordinata di cellule ai vari destini lungo la stria primitiva. Questo lavoro dimostra come il controllo negativo sulle funzioni delle Smad da parte di Ecto sia una componente fondamentale del meccanismo di lettura da parte delle cellule dei segnali TGFβ.

PUBLICATIONS

Sirio Dupont, Anant Mamidi, Michelangelo Cordenonsi, Marco Montagner, Luca Zacchigna, Maddalena Adorno, Graziano Martello, Michael J Stinchfield, Sandra Soligo, **Leonardo Morsut**, Masafumi Inui, Stefano Moro, Nicola Modena, Francesco Argenton, Stuart J Newfeld, Stefano Piccolo, FAM/USP9x, a deubiquitinating enzyme essential for TGFβ signaling, controls Smad4 monoubiquitination. *Cell* 2009 vol. 136 (1) pp.123-35

Graziano Martello, Luca Zacchigna, Masafumi Inui, Marco Montagner, Maddalena Adorno, Anant Mamidi, **Leonardo Morsut**, Sandra Soligo, Uyen Tran, Sirio Dupont, Michelangelo Cordenonsi, Oliver Wessely, Stefano Piccolo MicroRNA control of Nodal signaling, *Nature* 2007 vol. 449 (7159) pp. 183-8.

This was realized with the main contributions from the colleagues Dr. Sirio Dupont and Dr. Michelangelo Cordenonsi who provided key scientific advices. I primarily contributed to the generation of compound mutants and their phenotypic characterization. Dr. Regine Losson's lab at the Institut de Génétique et de Biologie Moléculaire et Cellulaire (IGBMC) generated the heterozygous mice (Ecto+/-).

INTRODUCTION

Anatomy of early mouse development

Mouse embryonic development lasts approximately 19 days from conception to delivery. During the first days post coitum (dpc) the embryo is floating in the uterine cavity; then, at E4.25 (i.e. at 4.25 dpc), the embryo implants in the uterine wall. This event marks the beginning of proper embryo development as well as the beginning of the maternal-fetal exchange system formation.

Already before implantation, differentiative events take place in the mouse embryo. After the first cell divisions that bring the fertilized egg to the morula stage, the embryo undergoes a morphological compaction originating a hollow spherical structure called blastocyst. The first differentiative events in mouse development occur during these early stages. In fact, in the blastocyst we can identify two main cell types: the trophectoderm (the outside layer) and the inner cell mass (ICM, a small cell mass inside the blastocyst cavity) (Fig. 1a).

The trophectoderm cells are themselves differentiated, since we distinguish polar trophectoderm that is associated to ICM, and mural trophectoderm that surrounds the rest of the blastocoel (the blastocyst cavity).

The ICM itself is rapidly going to differentiate, originating a layer directly exposed to the blastocoel, the primitive endoderm (the hypoblast in humans and chicks), and epiblast, which is now between primitive endoderm and polar trophectoderm. Primitive endoderm will give rise to two cell lineages: visceral endoderm (VE) that will sustain directly ICM growth, and parietal endoderm that will migrate to adhere to mural trophectoderm. This is the structure that undergoes implantation at around E4.25; note that this structure has an axial symmetry that defines the first embryonic axis, and that is dictated by the site of ICM location inside the blastocoel (Fig. 1b).

The implanted blastocyst rapidly undergoes several architectural changes. The blastocyst elongates along its axis, which is called from now on the proximo-distal axis (P-D). This elongation is mediated by the growth of the epiblast at the distal pole and by the growth of polar trophectoderm at the proximal pole; in particular the polar trophectoderm grows towards the epiblast, giving rise to a column of cells that are called extraembryonic ectoderm (EXE), which are in direct contact with the epiblast. These proliferation events originate an ellipsoid-like structure that fills up the blastocoel: the egg cylinder. In the egg cylinder before gastrulation, the pluripotent cells that will give rise to the embryo proper are well confined in the epiblast; these cells organize themselves in a cup-shaped epithelial sheet, whose proximal rim directly confines with the EXE. At this stage, the embryo is inside the former blastocoel, which is now called the yolk sac cavity; the epiblast, through the process of cavitation, originate itself a unique inner cavity, the proamniotic cavity, which is surrounded by epiblast and EXE (Fig. 1c,d).

Gastrulation, the hallmark of metazoan development, starts in the mouse at E6.5. Gastrulation initiation is marked by mesoderm induction at a specific site in the proximal epiblast (Fig. 1e). This asymmetric event accomplishes, among several other things, the formation of the first body axis of the embryo proper that is the antero-posterior axis, the posterior being the site of the mesoderm induction event. Morphologically, mesoderm induction originates a structure called primitive streak, which starts to elongate from the proximal to the distal end of the epiblast. Mesoderm cells originate from the epiblast (Fig. 2a), but then lose epithelial features and starts migrating and acquiring mesenchimal features; these cells invaginate between epiblast and visceral endoderm, and migrate extensively, giving rise to mesoderm (which will surround all the epiblast) and definitive endoderm (which will egress into the outer layer and intercalate with the primitive endoderm). The most distal part of the primitive streak, which is the most anterior one, originates the Node, the mammalian organizer tissue (Fig. 2b). Mouse embryo retains an overall cup shape across gastrulation, when it transforms from a bilaminar (epiblast + visceral endoderm) to a trilaminar structure (epiblast + mesoderm + definitive endoderm) (Fig. 2a,b).

The Node has organizing capabilities, and orchestrates the further development of the mouse embryo. The Node is localized at the distal tip of gastrulating embryo, and is composed by two sheets of cells, one of which is directly exposed at the outside space (Fig. 2c,d). From this discoid structure emanates directly a column of cells called the anterior mesendoderm (AME, also known as notochordal plate or prechordal plate); the AME will elaborate the axial structure of the late embryo. The AME is itself a two layered elongated structure, being composed of an inner neuro-ectoderm layer and an outer mesendoderm layer, composed of small spherical cells, which are in direct continuity with the endoderm cells (Fig. 2d). This is the most anterior structure organized from the Node, and will later profoundly influence the patterning of neural tissue along the second body axis of the embryo proper, the dorso-ventral axis.

At the posterior pole gastrulation proceeds with the deposition of new endoderm, mesoderm and neuro-ectoderm derivatives, that will aggregate in the formation of body segments (Tam and Loebel, 2007; Tam et al., 2006).

The TGFβ signaling pathway

Cells' behaviors (proliferation, differentiation, organization within a tissue, metabolism, death) rely on information networks; this information must be transduced from the extracellular space to the nucleus in order to be integrated into coherent genetic programs. Among the stimuli that can signal to the cell surface there is the Transforming Growth Factor-β (TGFβ) family, a large group of cytokines important in a variety of cellular contexts from body axis formation, left-right patterning and organogenesis in the embryo to tumor suppression, immune surveillance, cellular homeostasis and differentiation in adult tissues. The loss of this control leads to aberrant cell behaviors contributing to the development of cancer and inborn defects (Derynck et al., 2001; Massague, 2000; Wakefield and Roberts, 2002) .

The TGFβ family consists of more than 40 members that can be divided into two main branches: one comprises TGFβs, Activins, Leftys and Nodals, while the other is made of BMP ligands and Anti-Mullerian hormone. The signaling pathway of the TGFβ family from the ligands to the target genes is well established (Fig. 3a). The secreted, latent, precursor is cleaved by enzymes, such as furins, and the bioactive cytokine forms a dimer that bridges together two pairs of receptor serine-threonine kinases, known as Type I and Type II receptors. Each ligand of the TGFβ family binds to a specific Type I/Type II receptor couple; the main function of Type II Receptor is to activate Type I Receptor, which in turn activates cytoplasmic Receptor-Smads proteins through phosphorylation in the C-terminal domain. Activated R-Smads form a complex with Smad4, common to all R-Smads, and shuttles to the nucleus where they can activate or repress their target genes.

The specificity of the response to a TGFβ ligand is determined by the ligand itself and by the cellular context. Each of the two main branches of TGFβ family has specific R-Smads: the TGFβ subfamily signals through Smad2 and Smad3 while the BMP subfamily through Smad1 and Smad5. R-Smads of the two different groups are able to activate different sets of target genes, giving to the cellular response a first round of specificity. However this step is largely insufficient to explain the complexity and the diversity of each cellular response to TGFβ signaling. How can this pathway be so pleiotropic and yet specific? The answer must be found in the low affinity of R-Smad/Smad4 complex for its DNA recognition site (CAGAC). This feature forces the complex to associate with additional cofactors in order to achieve binding with high affinity, and thus specificity, to target genes. In this way TGFβ pathway can integrate signals coming from other pathways, or stimuli, that can modify and modulate Smad cofactors. Each cell, in each context, exhibits a particular set of Smad transcriptional partners, providing a suitable background for the correct TGFβ-activated transcriptional response.

As outlined above, the cascade transduces the signal with just a couple of steps from the extracellular space to gene transcription. As the development field shows very well, the responses triggered by TGFβ is not only cell type specific, but also dependent on the duration and on the strength of the signal itself. During embryonic development TGFβ molecules work as morphogens: they induce differentiation of cells towards distinct types according to the ligand concentration and/or the time of exposure. In order to attain such a fine-grained signaling, clearance systems must be in place in order to let the time of exposure to ligands to be transduced correctly. In other words, if Smad activity must be proportional to the ligand quantity and readily tuned by variations of extracellular ligand availability, systems must be in place to avoid saturation and allow transduction to be shut off if the ligand is not present anymore. The presence of these systems as an integral component of the pathway potentially adds a new layer of control over the pathway outcome, yet a largely unexplored one. Tuning the inhibition systems allows cells to tune the signal transduction itself: this paves the way for cross-talk with other pathways and also the possibility to use this regulation compartment as a target for medical purposes.

One example of this kind of control mechanism is the phosphorylation/dephosphorylation cycle receptor Smads undergo. R-Smads are phosphorylated (and hence activated) by ligand activated receptors, and are then dephosphorylated (hence inactivated) by specific phosphatases in the cell nucleus (Lin et al., 2006; Schmierer and Hill, 2005). In this way, R-Smads are constantly forced by phosphatases to exit the nucleus and check the activity status of the receptors.

We have recently proposed another layer of control of this type (Dupont et al., 2009); in this case it is a cycle of monoubiquitination/deubiquitination that sustains the regulation (see below for details), and the target component of the pathway is Smad4, the Co-Smad (Fig. 3b).

Ubiquitin-dependent regulation of TGFβ signaling

Ubiquitination has been discovered for its role in protein degradation, but in recent years several other mechanisms emerged by which ubiquitination can regulate protein function, including regulation of subcellular localization, protein-protein interactions and activity (Salmena and Pandolfi, 2007). Just like phosphorylation, which is constantly opposed by dephosphorylation, ubiquitination is also a reversible modification, as indicated by the existence of a whole family of deubiquitinating enzymes (DUBs) (Nijman et al., 2005).

Ubiquitination occurs through a three-step process involving ubiquitin-activating (E1), ubiquitin-conjugating (E2), and ubiquitin ligase (E3) enzymes (Pickart, 2001). E3 ubiquitin ligases, which are generally thought to give specificity to the system, are divided into three classes based on their structure: HECT (homologous to the E6-associated protein C-terminus) type, RING (really interesting gene) type, and U-box type (Pickart, 2001). The major difference between these proteins is that HECT-type ligases form a covalent intermediate with Ub, while the others only recruit E2 enzymes to the substrate.

Ubiquitination is oppositely regulated by ubiquitin cleavage, which is performed by deubiquitylating enzymes (DUBs). The human genome encodes for approximately 100 DUBs, which can be divided into five classes on the basis of differences in the catalytic domain (Amerik and Hochstrasser, 2004; Nijman et al., 2005).

Isolation of several TGFβ regulators endowed with Ub-ligase activity unveiled how TGFβ pathway is extensively regulated by ubiquitination, both positively and negatively (Izzi and Attisano, 2006). The first Ubiquitin-ligase isolated in the pathway was Smurf1, the ligase responsible for Smad1 degradation, based on its anti-BMP activity in Xenopus embryos (Zhu et al., 1999). Subsequently, several other E3 has been proposed to regulate aspects of TGFβ signal transduction, although the physiological significance of most of these findings is still not clear.

Being a common intracellular effector of both TGFβ and BMP signaling pathways, Smad4 is a critical point at which both cascades can be modulated to maintain homeostasis. Like R-Smads, Smad4 has been proposed to be regulated by a number or E3 ubiquitin ligases including Smurf1/2, Nedd4-2, SCF/β -TrCP1 and WWP1/Tiul1 (Moren et al., 2005). However, because Smad4 lacks a PY motif, it cannot directly associate with HECT-containing E3 ligases, but rather can recruit the enzymes through adaptors such as I-Smads and R-Smads. Moreover, the endogenous requirement of these ligases for Smad4 regulation has not been addressed, questioning the physiological relevance of these biochemical observations. In our lab, we recently described another Smad4 ubiquitin ligase, Ectodermin/Tif1γ (Ecto) (Dupont et al., 2005). We have identified Ecto in a functional screen for ectoderm determinants in Xenopus embryos. Ectodermin protein is asymmetrically localized within the embryo, being enriched in the animal hemisphere where the ectoderm forms. In Xenopus, Ecto is essential for the specification of the ectoderm by fulfilling two functions: first it acts by restricting the mesoderm-inducing activity of TGFβ signals to the mesoderm, protecting ectodermal cells from TGFβ ligands emanating from the vegetal hemisphere into extracellular spaces. Second, it prevents excessive BMP signaling in the animal pole, thus allowing for the proper activity of BMP antagonists secreted by the Spemann Organizer, resulting in efficient neural induction (Dupont et al., 2005). Moreover, we showed that the function of Ectodermin as antagonist of TGFβ and BMP signals is conserved in human cells, representing a constitutive fence against TGFβ cytostatic effects. Mechanistically, we proposed that Ectodermin works as RING-finger ubiquitin ligase for Smad4, regulating Smad4 localization and possibly its stability.

By means of a siRNA screen we had identified also FAM (Usp9x), as a deubiquitinase (DUB) acting as essential and evolutionarily conserved component in TGFβ and BMP signaling. FAM/Usp9x, the homologue of Drosophila fat-facets (Wood et al., 1997), acts as a DUB critical for TGFβ and BMP responsiveness in human cells and Xenopus embryos. Biochemically, FAM interacts with and deubiquitinates monoubiquitinated Smad4, opposing the activity of Ectodermin/Tif1γ (Dupont et al., 2009). We propose that the cycle of ubiquitination/deubiquitination triggered by the Ecto/FAM pair is a fundamental mechanism cells use to control Smad4 activity (Fig. 3b).

Multiple roles of TGFβ ligands during early mouse development

During early mouse development, TGFβ ligands are able to coordinate growth and differentiation of the different cell lineages. The major ligand expressed in the early period is Nodal, and has a similar role in all mammals. In particular, in mouse embryo *Nodal* is expressed from blastocyst stage on; at E5.0 its transcript is clearly detectable in all the epiblast and surrounding visceral endoderm cells (Collignon et al., 1996; Varlet et al., 1997) (Fig. 4a). Nodal signaling through the canonical Rmad/Smad4 pathway exerts pleiotropic functions in early mouse embryo; these functions are cell lineage specific and strictly temporally controlled.

The first known role of Nodal is to maintain the epiblast in an undifferentiated state through a self-sustaining positive feedback loop; this is accomplished by maintaining the transcription of a cocktail of transcription factors (*Oct4*, *Sox2*, *Nanog*) that sustain the stem features of the epiblast. In facts, the epiblast of *Nodal* and *Smad4* deficient embryos, as well as depleted ES cells, display an abnormal differentiation towards the neuroectoderm lineage (Camus et al., 2006; Pfister et al., 2007; Rodriguez et al., 2007).

At a strictly timed stage (E5.5), Nodal induces anterior visceral endoderm (AVE), a specialized subpopulation of visceral endoderm cells initially found at the distal tip of the embryo (Fig. 4a). These extraembryonic cells express specific Nodal target genes (such as *Cerl*, *Lim1* and many others), which are commonly used to identify this subpopulation of cells from the surrounding visceral endoderm cells. The AVE then rotates (E6.0) towards the prospective anterior pole of the embryo, in a Nodal-dependent manner. Thus, from a marker genes point of view, AVE rotation is the very first event that establishes the anterior pole of the antero-posterior axis in the mouse embryo; mesoderm induction, in facts, will occur later (E6.5) at the opposite side, marking the posterior pole (Fig. 4a).

The relevance of the Nodal/Smads pathway in the establishment of the early mouse embryo body plan is strongly supported by many genetic studies:

- in *Nodal* knockout embryos AVE specific genes are not detectable (Collignon et al., 1996; Norris et al., 2002; Varlet et al., 1997) (Fig. 4b);
- in the AVE, Nodal induced target genes activation requires Smad4, since *Smad4* knockout embryos are early embryonic lethal, but these defects are rescued with wild type extraembryonic lineages (Chu et al., 2004; Sirard et al., 1998; Yang et al., 1998);
- similarily, Smad2 (one of the TGFβ specific R-Smad), is required in visceral endoderm for AVE induction (Dunn et al., 2005; Dunn et al., 2004; Tremblay et al., 2000; Waldrip et al., 1998) (Fig. 4b);
- mice with reduced Nodal signaling strength do induce AVE specific genes, but the subsequent AVE rotation is impaired; this happens in *Cripto* knockout embryos, which lack the Nodal co-receptor Cripto (Ding et al., 1998; Kimura et al., 2001), and in embryo with a reduced Nodal ligand dosage (the Nodal allele used in this study displays an inactive feedforward loop

enhancer) (Brennan et al., 2001; Norris et al., 2002; Varlet et al., 1997; Vincent et al., 2003). In these embryos, the AVE genes are induced at the distal tip, but they do not rotate to the prospective anterior side (Fig. 4b).

The relevance of Nodal signaling in the pre-gastrulation (i.e. before E6.5) mouse embryo is extensive, since it signals also to the other extraembryonic lineage of the early mouse embryo, the trophoblast (Ang and Constam, 2004). It is thought that Nodal signals to the trophoblast to maintain it throughout gastrulation. This effect is at least in part indirect through FGF4; in facts, Nodal is indispensable for the expression of *FGF4* in the epiblast, from where FGF4 itself directly signals to the trophoblast cells, to induce and maintain their stemness features. *Nodal-/-* embryos display initial activation of trophoblast stem cell specific genes at E5.5 to E6.0, but then this tissue seems not to be correctly sustained, since these trophoblast specific genes are not maintained. This is paralleled by the reduction of FGF4 in the epiblast, which is thought to be the direct effect of *Nodal* removal. Indeed, the trophoblast cells of *Nodal-/-* embryos seem to be freezed in an intermediate stage of differentiation, because they express transient-amplifying specific genes but not stem cell specific genes (Brennan et al., 2001; Guzman-Ayala et al., 2004; Lu and Robertson, 2004; Mesnard et al., 2006). Whether Nodal has a direct signaling function to trophoblast cells is still unknown (see also Fig. 13b for our proposed model).

Many of the results that support this view come from studies executed using trophoblast stem (TS) cells; these cells can be isolated from blastocysts or early egg cylinder embryos, and have been extensively characterized in vitro from a differentiation and transcription factors point of view. TS cells grow in a stem-like manner in the presence of FGF4 in the medium; upon removal of FGF4, these cells undergo differentiation towards terminally differentiating trophoblast cell types. In this way it has been shown that this in vitro system recapitulates the trophoblast development from a marker and a cell cycle point of view (Tanaka et al., 1998), thus coupling the advantage of in vitro manipulation with good resemblance of the in vivo counterpart. As such, the analysis of TS cells from a signals point of view is still scarce, and awaits deeper investigations.

At streak stages (from E6.5 on), Nodal has a major role in the induction and patterning of the nascent mesoderm (Fig. 4a,b). In particular, it is a gradient of Nodal activity that patterns the primitive streak along its antero-posterior axis (Dunn et al., 2004; Lowe et al., 2001; Lu and Robertson, 2004; Vincent et al., 2003). The gradient of Nodal activity is able to specify anterior fates at peak signaling levels, whereas it induces posterior fates at lower signaling levels. In this context, what is known is that Smad4 is required for specifying anteriormost fates, namely for the formation of the anterior primitive streak and node (Chu et al., 2004) (Fig. 4b).

Interestingly, the many Nodal functions in early mouse embryo are not uncoordinated or randomly executed. On the contrary, Nodal signaling seamlessly orchestrates the maintenance or restriction of embryonic pluripotency and establishes the body plan. At early stages, Nodal sustain the amplification of pluripotent cells, acting as a growth factors for the epiblast; this is fundamental for the embryo to reach gastrulation with the right balancing of the lineages, thus allowing germ layers to be correctly induced. As development proceeds, Nodal patterns the extraembryonic tissues (visceral endoderm and trophoblast); this accomplishes a double-faced aim: differentiate the tissue that will allow the formation of the embryo-to-mother exchange systems (the very first duty for mammalian embryos), and instruct the early signaling center with the correct interpretational keys able to pattern the whole conceptus. One key event is AVE induction; with this event, at a pole of the only morphological axis present so far (the proximo-distal axis), specific Nodal target genes are induced; this event marks the beginning of the formation of the first body axis marked by differential gene expression, the antero-posterior axis. The distal tip of the early embryo, where the AVE forms, will in facts migrate and become the anterior pole of the pregastrula stage mouse embryo.

The AVE specific genes, induced by Nodal, play a central part in this coordinate cascade of events. In facts, besides AVE specific transcription factors, AVE cells start expressing *Cerberus* and *Lefty1* (Fig.4) that are secreted molecules that inhibits Nodal itself. These molecules serve two main goals:

1. limits the effects of Nodal on itself; in facts, the primary stimulus to *Nodal* transcription is Nodal ligand itself; this happens through a strong feedforward loop that uses the canonical pathway from ligand to an enhancer in the intronic promoter region of the *Nodal* gene, as well as of *Cripto* gene (Ben-Haim et al., 2006). This loop helps Nodal function, but needs tight control in order not to explode. This is accomplished using a negative feedback circuit, which is a well known control mechanism. In this case, Nodal induces its own antagonists, which in turn reduce *Nodal* expression (Fig. 4a). In agreement with this model, the double knockout embryos for *Cerberus* and *Lefty1* display the consequence of an enhanced Nodal activity in the epiblast: loss of primitive streak patterning and emergence of ectopic primitive streak (Perea-Gomez et al., 2002).
2. restricts the effect of Nodal on epiblast cells at the prospective posterior pole; with its migration, AVE creates a Nodal-free zone at the distal tip and at the anterior side of the embryo, a fundamental condition for head development (Piccolo et al., 1999). On the other hand, the region of the epiblast that is more far from the AVE will be the zone where Nodal is less inhibited, and thus more expressed and active (thanks to the feedforward loop). It is in this region that Nodal induces the mesoderm master genes *T* (*Brachyury*), *Wnt3a*, *Eomes* and others (Arnold and Robertson, 2009), in a small group of epiblast cells; mesoderm ingression will mark the formation of primitive streak and thus the beginning of gastrulation.

Nodal role on trophoblast cells is in agreement with the same logic. In the trophoblast, Nodal sustains the development of a fundamental tissue for the subsequent development of the conceptus; this effect is thought to be indirect, through the activation by Nodal of *FGF4* in the epiblast. By sustaining trophoblast development, Nodal reaches two aims:

a) coordinating the patterning of the embryo. In facts, the trophoblast tissue serves also as a source of patterning signals for the whole embryo; in particular, Nodal sustains *Bmp4* expression in the EXE. Bmp4 is another TGFβ family member that is, among several other things, fundamental for inhibition of neural fates in the epiblast cells. Moreover, Bmp4 presence is required as a support for Nodal during mesoderm induction (Ben-Haim et al., 2006);

b) sustaining Nodal activity itself. The trophoblast cells are in facts the source of secreted proteases (Spc4 and Spc2) that cleave Nodal protein in the extracellular space, turning the ligand from the inactive (pro-Nodal) into its active (Nodal) form (Constam and Robertson, 2000).

Interestingly, Nodal patterning signals before gastrulation are directed towards extraembryonic tissues. This is the only possibility for the mammalian embryo to start the patterning as soon as possible. In facts, before gastrulation, epiblast cells start a proliferative phase of massive growth, during which extensive cell mixing moves cells and establish new and tenuous cell-cell contacts (Tam et al., 2006). It is impossible to instruct a group of cells able to organize neighboring cells in such an astir landscape. On the contrary, extraembryonic tissues do proliferate in a strictly controlled and coherently clonal manner. In this situation, it is clear why Nodal signals initially to the extraembryonic tissues, in order to instruct signaling centers that are able to start a cascade that will eventually pattern the whole mouse embryo.

RESULTS

Ecto homozygous mutant embryos display profound defects in polarity and patterning before gastrulation

To investigate the role of Ecto in vivo, we generated *Ecto* conditional and germ-line knockout alleles (Fig. 5a). Mice heterozygous for the *Ecto* null mutation (*Ecto*+/-) were viable and fertile; however, homozygosity resulted in embryonic lethality. Indeed, embryos from heterozygote intercrosses were collected at different stages of gestation and *Ecto* mutants could be recovered at the expected Mendelian ratios at E5.5 through E7.5, but not at later stages. Morphological and histological analyses demonstrated that *Ecto* mutants display striking defects in embryonic polarity and tissue patterning. When compared to control littermates, E6.5 *Ecto* mutants were smaller and lacked a clear distinction between epiblast and Extraembryonic Ectoderm (EXE). Wild-type embryos formed mesoderm as a consequence of gastrulation; in contrast, *Ecto* mutants could readily be identified by the undivided proamniotic cavity and the lack of a primitive streak (Fig. 5b). Defective mesoderm formation was confirmed by in situ hybridization at early streak stage examining the expression of markers, such as *T*, *Eomes* and *Wnt3* (Fig. 6). These data indicate that *Ecto* is required for mouse gastrulation.

As the pregastrulation development of extraembryonic tissues relies on the activity of early-acting Nodal/Smad4 signaling (Arnold and Robertson, 2009), we tested if defects in *Ecto* mutants initiated with abnormal extraembryonic development. Expression of AVE markers at E5.5 was strikingly upregulated in *Ecto* mutants: when these markers were barely detectable in wild-type littermates, signals of the Nodal targets *Cerberus-like* (*Cerl*) and *Lefty1* mRNAs were massive in knockout embryos, becoming rapidly saturated in an abnormally broad AVE domain (Fig. 7a). While in E6.5 wild-type embryos AVE markers are usually restricted to an anterior narrow stripe of cells, in *Ecto* mutants robust *Cerl* and *Lim1* expression was vastly expanded around the epiblast (Fig. 7b). These results support a model in which Nodal induces AVE and Ecto restrains this Nodal function (Fig. 7c).

Defective AVE patterning in *Ecto* mutants is a cell autonomous defect

Genetic evidences indicate that AVE responds to Nodal ligands emanating from the epiblast (Lu and Robertson, 2004). Thus, we next challenged the notion that AVE expansion is caused by a cell-autonomous enhanced Smad responsiveness as opposed to being secondary to increased ligand expression/availability in the epiblast. The latter hypothesis is based on the Nodal feedforward autoregolatory loop, which could lead to an increase in Nodal ligand availability. To this end, we made use of the paternally-inherited *Sox2-Cre* transgene, recombining the *Ecto* conditional allele in the epiblast lineage specifically (*Sox2-Cre; Ecto fl/-* embryos, hereafter *Ecto-EpiKO* or *EpiKO*). In these *EpiKO* mutants, a genetically wild-type AVE did not display any of the abnormalities characterizing the *Ecto* germline mutants, as *Cerl* and *Lefty1* mRNAs were comparable in localization and intensity to wild-type embryos (Fig. 10a). In line, at E5.5, *Nodal* is expressed normally in *Ecto* mutant embryos (Fig. 10b) and, by immunofluorescence, Smad2 phosphorylation is comparable between wild-type and *Ecto* mutants (Fig. 10c). Thus, *Ecto* is required cell-autonomously to restrain Nodal responsiveness, downstream of Nodal production and Smad2 phosphorylation.

AVE expansion in *Ecto* mutants is mediated by Smad4

The AVE phenotype of *Ecto-/-* embryos is unprecedented and is opposite to those reported for *Nodal*, *Smad2* and *Smad4* knockouts (Brennan et al., 2001; Waldrip et al., 1998; Yang et al., 1998). Hence, we investigated the genetic relationships between *Ecto* and its biochemical target *Smad4* (Dupont et al., 2009). We analyzed embryos from crosses of mice carrying the floxed alleles for the two genes (*Ecto fl/-* and *Smad4 fl/-*) that were undergoing zygotic deletion in the *CAG-Cre* maternal background. *Ecto fl/-;CAG-Cre* embryos were indistinguishable from *Ecto* germline homozygous mutants (compare Fig. 9a with Fig. 7a) and *Smad4 fl/-;CAG-Cre* phenocopied morphologically the previously reported defects of the null-allele (Yang et al., 1998). Extending these studies, we found that *Smad4* is dispensable for VE specification (as revealed by the detection of the *AFP* marker, Fig. 9b), but required for *Cerl* and *Lim1* induction (Fig. 9a). Remarkably, embryos double mutants for *Smad4* and *Ecto* were indistinguishable from *Smad4* mutants (Fig. 9a and b). Thus, *Smad4* is an obligate mediator of *Ecto* activity.

AVE defects in *Ecto-/-* embryos are due to unrestrained Nodal signaling

Data presented so far suggest that disruption of the Ecto/Smad4 inhibitory axis leads to excessive Nodal responsiveness in AVE. If so, this should be rebalanced by a concomitant reduction of the Nodal dosage. To this end, we combined *Ecto* mutant with a strong *Nodal* hypomorph (Norris et al., 2002) (*NodalΔ600/-*), leading to a remarkable rescue of AVE patterning (Fig. 10a). This indicates that the AVE phenotype in *Ecto* mutants is due to enhanced Nodal signaling.

As previously reported (Norris et al., 2002), low levels of Nodal expression in *NodalΔ600/-* were per se often insufficient for AVE rotation; notably, however, in the *Ecto-/-; NodalΔ600/-* compound mutants the AVE invariably rotates (Fig. 10c). Thus, lowering the Nodal dosage in *Ecto* mutants compensates an exalted Smad intracellular responsiveness and viceversa.

These results suggests that, in vivo, the net activity of Nodal/TGFβ is the result of two components: extracellular ligand availability and negative control of over Smad responsiveness; the loss of negative control of responsiveness in *Ecto* mutants profoundly alters embryonic patterning, but these defects are normalized by reduction of Nodal ligand availability (Fig. 10b).

Ecto maintains the trophoblast compartment by opposing Nodal signaling

Next, we characterized molecularly the development of the other extraembryonic tissue, the trophoblast lineage, in *Ecto* mutants. As shown in Fig. 11a, the trophoblast stem (TS) cells and EXE markers *Eomes*, *Cdx2* and *BMP4* were undetectable in E5.5 *Ecto-/-* embryos. This represents a cell-autonomous requirement as *Ecto-EpiKO* embryos displayed normal EXE development (Fig. 11c). Lack of EXE in *Ecto* mutants is paradoxically similar to the phenotype of *Nodal* mutants (Brennan et al., 2001); however, in the case of *Nodal*, this is secondary to defective Epiblast patterning as Nodal sustains *Oct4* and *FGF4* transcription in the epiblast, which, in turn, maintains TS self-renewal (Guzman-Ayala et al., 2004; Lu and Robertson, 2004; Mesnard et al., 2006). In contrast, *FGF4* and *Oct4* are normally expressed in *Ecto* mutants (Fig. 11b).

Strikingly, Nodal attenuation rescued the EXE phenotype of *Ecto* mutants, as *Eomes* and *BMP4* transcripts were invariably rescued in combined *Ecto-/-; NodalΔ600/-* or *Ecto-/-; Nodal+/-* embryos (Fig. 11d for *BMP4* expression, see Fig. 14 for *Eomes*). Taken together, these data strongly suggest that *Ecto* protects the TS lineage from excessive Nodal signaling.

Ecto maintains EXE self-renewal

To understand the nature of *Ecto* role in EXE, we monitored TS induction from earlier developmental stages. At the late blastocyst stage, *Cdx2* was normally expressed in *Ecto* mutants (Fig. 12a) indicating that excess of Nodal responsiveness affects later events. We then monitored cell viability, but wild-type and mutant embryos showed comparable apoptosis and proliferation rates (Fig. 13a). As development proceeds, we found that *Ecto* mutants do retain expression of *SPC4* and *Pem*, identifying the presence of more differentiated cells of the ectoplacental cone (Constam and Robertson, 2000; Lin et al., 1994), but lose expression of *Mash2*, a marker for transit amplifying trophoblast progenitors (Guillemot et al., 1995) (Fig. 12a). This differs from *Nodal* mutants where *Mash2* expression is enhanced (Guzman-Ayala et al., 2004). These data suggest that, in addition to its role in the epiblast for *FGF4* expression, Nodal signaling plays an earlier and likely direct role on trophoblast cells, promoting their differentiation.

Ecto prevents Nodal-induced differentiation of trophoblast stem cells

To validate the hypothesis of a direct role of Nodal on trophoblast differentiation, we established Control (shGFP) and Ecto-depleted (shEcto) mouse TS populations by lentiviral infection (Fig. 12b), and compared them for the expression of stem and differentiation markers (Fig. 12c). When cultured in stemness/proliferating medium, Control and shEcto TS cells were comparable in terms of marker expressions and cell cycle profile, reinforcing the notion that *Ecto* is not required for TS cells induction or self-renewal. However, once TS cells were induced to differentiate, in the presence of the Nodal-related ligand Activin shEcto cells specifically displayed a robust increase in the expression of differentiation markers *4311* (Tanaka et al., 1998) and *Gcm-1* (Anson-Cartwright et al., 2000) (Fig. 12c), recapitulating in vitro our observations on *Ecto* mutants. Tight control over Nodal activity is thus critical for balancing stem cells renewal and differentiation in the trophoblast lineage; in *Ecto* mutants, uncontrolled Nodal signaling causes wholesale exhaustion of the stem cell pool (Fig. 13b).

These results point at a novel role for Nodal in inducing differentiation in the early trophoblast compartment; this function of Nodal is normally opposed by *Ecto* (Fig. 13b). Thus, Nodal exerts morphogenetic properties also in the trophoblast compartment (Fig. 13c).

Lack of mesoderm in *Ecto* mutants is caused by excessive Nodal and defective EXE development

By losing the EXE, *Ecto* mutants are deprived of an essential source of mesoderm inducing and patterning signals (Arnold and Robertson, 2009); at the same time, they display a massive expression of Nodal antagonists, such as *Cerberus* and *Lefty*. This raises questions on what is the primary cause of defective mesoderm in *Ecto* mutants. Remarkably, attenuation of Nodal signaling in compound *Ecto/Nodal* mutants also rescues mesoderm development, as revealed by transcription of the pan-mesodermal markers *Eomes* and *T* at the early gastrula stage (Fig. 14). Importantly, while the combination *Ecto-/-; NodalΔ600/-* rescues EXE, mesoderm and AVE (Fig. 10a, 11d, 14), compound *Ecto-/-; Nodal+/-* could rescue EXE and mesoderm but not AVE (compare red boxed pictures in Fig. 14), revealing that lack of mesoderm in *Ecto* mutants is primarily due to lack of EXE, and that this may be uncoupled from exalted AVE activity.

A further complicating issue is the fact that AVE and EXE development might be linked, as the EXE has also been proposed to secrete AVE inhibiting factors (Rodriguez et al., 2005; Yamamoto et al., 2009). Is then the AVE expansion observed in *Ecto* mutants due to loss of EXE?

Our results suggest that this is not the case, as *Ecto-/-; Nodal +/-* embryos display rescued EXE in the presence of a still expanded AVE (Fig. 14, red box). Thus, the two events seem uncoupled, and expanded AVE in *Ecto* mutants is primarily due to enhanced Nodal responsiveness of the visceral endoderm (Fig. 14).

Ecto expression is patterned before gastrulation, Ecto activity is patterned after mesoderm induction

The *Sox2-Cre; Ecto fl/-* embryos (*Ecto-EpiKO*) allow to study more directly the role of *Ecto* in the epiblast, bypassing its early requirements in extraembryonic tissues, and likely allowing us to monitor post-gastrulation defects. It seemed interesting, since we monitored the localization of Ecto protein by immunofluorescence, and we found that it is expressed at higher levels in epiblast nuclei than in extraembryonic cells (Fig. 15a). This differential enrichment is particularly sharp at E5.5 but declines as development proceeds, with Ecto becoming ubiquitous during gastrulation.

Previous work established that a gradient of Nodal activity patterns the primitive streak (Dunn et al., 2004; Lowe et al., 2001; Vincent et al., 2003); in this context, *Smad4* is primarily required for peak signaling levels, namely, for the formation of the anterior primitive streak and node, marked by *FoxA2* expression (Chu et al., 2004). Being Smad4 a ubiquitous protein, and not directly controlled by TGFβ ligands, such localized and qualitative requirements remain unexplained. Ecto is required for Smad4 monoubiquitination, preventing the incorporation of Smad4 into Smad transcriptional complexes (Dupont et al., 2009); we therefore tested whether a patterned Ecto activity contributed to regionalize Smad4 activity in vivo. By means of anti-ubiquitin immunoprecipitations from embryonic lysates, followed by antiSmad4 western blotting, we found that, intriguingly, endogenous Smad4 is preferentially ubiquitinated in the proximal, but not distal half of the gastrulating embryo (Fig. 15b).

Massive Organizer induction in epiblast-specific *Ecto* mutants (*EpiKO*)

This raised the possibility that *Ecto* works to prevent excessive, if not precocious, Nodal/Smad4 signaling in proximal epiblast. Strikingly, we found that approximately a third of the

Ecto-EpiKO embryos displayed at streak stages an expanded *FoxA2* expression (Fig. 15c). These embryos appeared smaller and lacked an overtly elongated streak, and likely failed to undergo proper gastrulation. At later stages, *Ecto-EpiKO* embryos displayed a severely abnormal morphogenesis, highlighted by an expanded node and aberrant morphogenetic movements, in some cases leading to the growth within the amniotic cavity of a column of epiblast cells contiguous to the node rim. When node-derivatives were analyzed molecularly, surviving *Ecto-EpiKO* embryos showed expansion of the Node (marked by *FoxA2* staining, Fig. 15d), an almost radial expansion of the definitive endoderm marker *Cerl* (Fig. 15e), as well as duplications of Node and anterior axial mesendoderm tissues (*T* and *Shh* in situs, Fig. 15f). Intriguingly, these defects stem, at least in part, from an early-onset expression of anterior primitive streak fates, as revealed by heterochronic expression of *FoxA2* in the epiblast at prestreak stages (Fig. 16a). The exalted Smad responsiveness of *Ecto-EpiKO* embryos is also suggested by the analysis of *Nodal* expression that, due to a potent feed-forward loop, is perhaps the best read-out of Nodal activity (Brennan et al., 2001). In *Ecto-EpiKO*, *Nodal* transcription starts normally at E5.5 but aberrantly engrosses during gastrulation (Fig. 16a).

Together, the data suggest that *Ecto* is essential to orchestrate intensity of Nodal/Smad4 responses for proper primitive streak development. These early defects of *Ecto-EpiKO* are such that loss of *Ecto* in epiblast cells is incompatible with subsequent development. Indeed, we could identify only few *Ecto-EpiKO* embryos at E10.0, displaying defective brain development and open neural folds.

DISCUSSION

The TGFβ cascade is a fundamental player in mammalian development and adult tissue homeostasis. Although TGFβ ligands are widely expressed in vertebrate tissues, they can elicit their effects in a strict temporally and spatially controlled manner. For the signal to reach only the appropriate cells and with the correct intensity, mechanisms must be in place to determine where and when cells must not respond to TGFβ. This layer of regulation is just as likely to play a fundamental role in defining cell fate than the signal itself; yet, little is known on factors that shape Smad responsiveness in vivo (Schmierer and Hill, 2005). In the mammalian embryo, the TGFβ-related Nodal ligand signals through Smads to act as morphogen; depending on the cellular context and developmental timing, Nodal signaling seamlessly orchestrates the maintenance or restriction of embryonic pluripotency and establishes the body plan (Arnold and Robertson, 2009; Tam and Loebel, 2007). However, whether extracellular gradients of Nodal ligand exist in mouse embryos is unclear; with this work, we explored the possibility that the morphogenetic properties of Nodal may rely on negative Smad regulation.

The mechanisms by which cells clear nuclear Smad activity are starting to emerge (Itoh and ten Dijke, 2007; Wrana, 2009). However, these mechanistic results are largely uncoupled by sound in vivo validation, as in the case of Smurfs protein: these molecules were originally identified as intracellular inhibitors of the TGFβ cascade (Zhu et al., 1999), but the corresponding knockout embryos have a phenotype linked to the planar cell polarity pathway (Narimatsu et al., 2009). With our work, we now provide the first genetic evidences indicating that key to the morphogenetic properties of Nodal is a negative, cell-autonomous Smad regulation operated by the Smad4 Ubiquitin-ligase Ectodermin (Dupont et al., 2005; Dupont et al., 2009). Even more surprisingly, our data unveil that the extracellular modulation of TGFβ ligands becomes irrelevant in the presence of unleashed intracellular Smad4 activity. In other words, it is Ecto that endows cells with distinct interpretational keys to an otherwise "monotonous" Nodal signal, enabling the correct "dosage" of Nodal responsiveness required for embryonic patterning.

Analysis of *Ecto* knockouts showed how loss of *Ecto* invariably "upgrades" Nodal responses to a high-threshold of activity in all the tissues of the early mouse embryo: this was true for known Nodal responses, such as Anterior Visceral Endoderm (AVE) induction, but also unveiled novel functions of Nodal in the differentiation of the trophoblast lineage. Indeed, in the visceral endoderm, unrestrained Nodal signaling causes an unprecedented expansion of the *Cerberus/Lefty* expressing AVE territory. This effect is *Smad4*-dependent, and can be rescued by reducing the dosage of Nodal. These results bring to the important conclusion that, in vivo, the net activity of Nodal/ TGFβ is the result of two components: extracellular ligand availability and, unprecedently, negative control of over Smad responsiveness; the sole loss of this second component in *Ecto* mutants is sufficient to profoundly alter embryonic patterning (Fig. 10b).

Unexpectedly, we found that the same concept also applies to the trophoblast: here, loss-of-*Ecto* promotes dramatic wholesale differentiation and rapid exhaustion of the trophoblast stem (TS) cell compartment, an effect that was again remarkably rescued by reducing the Nodal dosage. This was recapitulated in vitro, as TS cells lacking of Ecto undergo uncontrolled differentiation in response to TGFβ. In this way, we prove for the first time the relevance of Nodal morphogenetic activity in the trophoblast compartment (Fig. 13c).

These extraembryonic defects cause an early embryonic lethal phenotype, with no *Ecto* mutant embryos reaching gastrulation. To bypass this lethality, we used *Ecto* floxed alleles crossed to the epiblast *Sox2-Cre* deleter. This enabled us to uncover the role of *Ecto* in mesoderm patterning, where Nodal signaling acts classically as a morphogen, inducing anterior fates at the highest levels (Dunn et al., 2004; Lowe et al., 2001; Vincent et al., 2003). Strikingly, *Ecto* mutant embryos show expansion of *Smad4*-dependent anterior fates (Node/Organizer), extending to the whole primitive streak. Moreover, also the fraction of embryos passing this stage still develop largely expanded Organizer derivatives, such as duplication of the Node/prechordal plate, and radial expansion of the definitive endoderm.

Adding a further twist, we found that Ecto activity appears spatially regulated: at the endogenous level, we found Smad4 ubiquitinated, and thus inactive, in the proximal embryo (posterior mesoderm, whose development is in fact *Smad4*-independent); in contrast, Smad4 is free of ubiquitin, and thus fully active, in the most anterior segment of the primitive streak, where the Node will form in a *Smad4*-dependent way. In other words, a ubiquitination-mediated patterning mechanism is shown to be essential to generate the "landscape" of TGFβ responsiveness, playing an equal if not superior role to extracellular ligand distribution. Thus, during gastrulation, the Nodal "morphogenetic gradient" is actually not a simple extracellular gradient of ligands, but is mainly mediated by negative Smad regulation (Fig. 16b-d).

Our previous studies indicated a function for Ectodermin as a general inhibitor of both TGFβ and BMP responses (Dupont et al., 2009; Dupont et al., 2005). It was therefore surprising to observe mainly Nodal-related phenotypes in *Ecto* mutant embryos. We reasoned that this might simply reflect the high degree of overlap between Nodal and BMP signaling in early mouse embryos (Ben-Haim et al., 2006; Di-Gregorio et al., 2007; Yamamoto et al., 2009); more intriguingly, this might highlight an intrinsic difference in their regulatory logic, with BMP signaling being mostly regulated in the extracellular space, and Nodal relying more on intracellular Smad regulation. Indeed, unleashing BMP activity leads to phenotypes profoundly different from those here described, as Chordin and Noggin double mutants embryos show reduced AVE and axial mesoderm (Bachiller et al., 2000).

An interesting possibility for future studies will be to determine whether Ecto activities are patterned by other signaling cues of the early embryo, or whether these might be exploited therapeutically in diseases characterized by excess of TGFβ activity, such as fibrosis or metastasis.

More than ten years of mouse knockouts for pathway activators (Smads and TGFβ receptors) have been essential to know what are the consequences of losing TGFβ responses; however, lack of appropriate genetic tools for Smad inhibitors left us blind on other equally central questions, namely, where, when and why cells must not respond to TGFβ. So far, no intracellular inhibitor of TGFβ signaling has received genetic support in corresponding knockout animals. This study shows how the *Ecto* mutants can be used to explore the uncharted territories of enhanced Nodal signaling during mouse embryonic development. With a stringent genetic analysis we strongly validated the model as being dependent on Smad4 activity and on enhanced Nodal signaling. It will be interesting to use this tool to answer the same questions in other contexts, for example during normal adult tissue homeostasis or in diseases.

EXPERIMENTAL PROCEDURES

Genotyping

Offsprings were genotyped by PCR on genomic tail DNA extracted by standard procedures (see Supplemental Table 1 for oligo sequences). After in situ, individual embryos were manually dissected with a tungsten wire (FineScienceTools) to eliminate the EXE and ectoplacental cone, thus avoiding maternal contaminations. Epiblast/VE tissues were lysed overnight at 55°C with mild agitation in 10mM Tris/HCl pH=8.0, 50mM KCl, 2mM MgCl2, 0,3% Tween-20, 0,5% NP-40 supplemented with fresh proteinaseK (Invitrogen, 1:40). Lysis volume was adjusted according to the stage: E5.5 20µl, E6.5 40µl. After vortexing, proteinaseK was inactivated 10min at 95°C, quenched on ice, and samples were centrifuged 10min/4°C/10000rcf. 4ul of the fresh supernatants were used for each PCR reaction using EX-Taq polymerase (Takara). For detection of the *Ecto-* allele in embryos of early stages, nested PCR was employed when necessary.

Generation of *Ecto* knockout and conditional alleles

To generate the Ecto/Tif1γ targeting vector, a genomic clone spanning exons 2, 3 and 4 was used (Yan et al., 2004). Briefly, a loxP flanked (floxed) PGK-Neo cassette was inserted within the first intron, and a third loxP site was inserted within the fourth intron (Fig. 5a). The targeting fragment was electroporated into 129/Sv H1 ES cells as described previously (Cammas et al., 2000). After selection, neomycin-resistant ES clones were expanded, and their genomic DNA was screened by PCR. Positive clones were further validated with Southern blotting analysis with two independent probes (not shown). ES cells bearing the correctly targeted allele were injected into C57BL/6 blastocysts to produce chimeric offspring. These were back-crossed with C57BL/6 mice, and their offspring was genotyped by PCR. Mice heterozygous for the targeted allele were then crossed with CMV-Cre transgenic mice (Dupe et al., 1997), and the offspring was analyzed by PCR to identify animals with either complete recombination of the loxP sites (null allele, *Ecto-*) or lacking of the PGK-Neo cassette due to recombination of the first and second loxP sites (conditional allele, *Ecto fl*). *Cre*-negative *Ecto*+/- and *Ecto fl/fl* mice were subsequently kept on a C57BL/6 background for phenotypic analyses. Animal care was in accordance with our institutional guidelines.

Generation of *Ecto-EpiKO* and compound *Ecto-/-;Smad4-/-* and *Ecto-/-;NodalΔ600/-* embryos

To obtain epiblast-specific *Ecto* knockout embryos, *Sox2-Cre; Ecto*+/- males were crossed with *Ecto fl/fl* females. In this setup the *Sox2-Cre* transgene selectively deletes the floxed alleles in ICM/epiblast cells (Hayashi et al., 2002). Embryos were genotyped after in situ hybridization for *Ecto fl*, *Ecto+*, *Ecto-*, and *Cre* alleles. Embryos were scored as mutants in the presence of *Cre*, *Ecto fl*, *Ecto-* and absence of *Ecto+* alleles.

To obtain embryos homozygous null for both *Ecto* and *Smad4*, *Ecto fl/fl;Smad4 fl/fl* (Bardeesy et al., 2006) males were crossed with *CAG-Cre; Ecto+/-; Smad4+/-* females. In this setup, the Cre protein supplied by the mother within the oocyte completely recombinates the paternal floxed alleles after fertilization, irrespective of transgene trasmission ((Sakai and Miyazaki, 1997) and our unpublished observations), raising the expected frequency of compound null embryos to 25%. Embryos were genotyped after in situ hybridization for *Ecto fl* (recognizing also the *Ecto+* allele), *Ecto-*, *Smad4 fl* (recognizing also the *Smad4+* allele), and *Smad4-* alleles. Embryos were scored as compound mutants in the presence of *Ecto-* and *Smad4-* and in the absence of *Ecto fl* and *Smad4 fl* alleles.

To obtain *Ecto-/-* embryos with reduced Nodal signaling, *Ecto+/-; Nodal+/-* (lacZ allele (Collignon et al., 1996)) mice were crossed with *Ecto+/-; Nodal+/Δ600* ((Norris et al., 2002) mice. Embryos were genotyped after in situ hybridization for *Ecto+*, *Ecto-*, *lacZ* and *NodalΔ600* alleles.

In situ hybridization

Mouse embryos were staged based on their morphology, considering the morning of the vaginal plug as E0.5. Embryos were manually dissected in ice-cold DEPC-treated phosphate-buffered saline (PBS) and fixed overnight in PBS 4% PFA at 4°C, dehydrated (for storage) and rehydrated through methanol series. Whole-mount in situ hybridizations were performed according to http://www.hhmi.ucla.edu/derobertis/ (Xenopus ISH protocol), with minor modifications to ensure efficient genotyping after staining: Day1, post-fixing after proteinaseK treatment was done with 4% PFA only, 1 hour at 4°C; Day3, washes were done with PBS 0,5% Goat Serum (GS, Invitrogen), without AP1 incubation before BM-Purple staining (Roche), and without post-fixation. Embryos were mounted in 80% glycerol and photographed with a Leica DMR microscope equipped with a Leica DC500 camera. For each experiment, at least 5 embryos of every genotype were analyzed.

Immunofluorescence and histology

For immunostaining, embryos were fixed overnight in PBS 4% PFA supplemented of phosphatase inhibitors (Sigma) at 4°C, dehydrated and rehydrated through methanol series. Embryos were permeabilized with two washes in PBS 0,5% NP40, 20min at 4°C, followed by one wash in PBS 0,3% TRITON X100, 20min at RT. After two washes in PBS 0,1% TRITON X100 (PBT), 15min at RT, embryos were blocked with two washes in PBT 10% GS, 1 hour at RT, and incubated overnight with rabbit anti-Ecto primary antibody (Sigma HPA004345, 1:75) in PBT 10% GS or rabbit mAb anti-phospho-Smad2 (CST-3108, 1:50) in PBT 3% BSA. The following day, embryos were washed twice in PBT 2% GS, 15min at 4°C, and five more times in PBT 2% GS, 1 hour at 4°C. Secondary Alexa555 goat anti-rabbit antibody (1:200) was incubated overnight in PBT 5% GS. The third day, embryos were washed five times in PBT, 15min at RT, mounted in 80% glycerol and photographed with a Nikon Eclipse E600 confocal microscope equipped with a Biorad Radiance2000 camera/laser scanning system. Nuclear localizations were confirmed by colocalization with YOYO1 staining (Invitrogen).

For histological analysis, deciduae were collected in PBS, fixed in Bouin's overnight, dehydrated, and embedded in paraffin. Serial sections were cut at 6µm and stained with Hematoxylin and Eosin according to standard procedures. Similar procedures were applied to obtain sections of embryos after in situ.

TS cell culture

TS cells were cultivated and passaged in feeder-free conditions as indicated in (Oda, Shiota 2006). pLKO lentiviral shRNA targeting mouse Ecto was purchased from Sigma (5'-CCGGCGTGTGATAGATTGACGTGTACTCGAGTACACGTCAATCTATCACACGTTTTT G-3'). Control shGFP sequence was as in (Adorno et al., 2009). Lentivirally-infected populations were established by puromycin selection as indicated in (Moffat et al., 2006). For differentiation assays, TS cells were seeded and grown in the same conditions for 2 days; differentiated samples were changed to DMEM 10% FCS (t=0) and cultivated for the indicated times, renewing the culture medium every two days. TGFβ stimulation was provided by adding every day 100ng/ml Activin-A (Peprotech) directly to the medium.

qPCR analysis

Cultures were harvested in Trizol (Invitrogen) for RNA extraction, and contaminant DNA was removed by DNAse treatment. Real-time qPCR analyses were carried out on triplicate samplings of retrotranscribed cDNAs with RG3000 Corbett Research thermal cycler and analyzed with Rotor-Gene Analysis6.1 software (see Supplemental Table 2 for oligonucleotides sequences). Experiments were performed at least twice, with duplicate biological replicates.

Immunoprecipitations and Western blotting

For the detection of endogenous Smad4 ubiquitination, 30 E6.5 wild-type mouse embryos were manually dissected using a pulled glass Pasteur pipette under the dissecting microscope to obtain the distal and proximal halves of the embryonic cup. Explants were harvested by sonication as in (Dupont et al., 2009). Lysates were supplemented of 0,5% SDS and boiled 5min, followed by 10x dilution with PBS. After immunoprecipitation with anti-Ubiquitin antibody (SantaCruz P4D1), 2 hours at 4°C, beads were washed three times with PBS 1% NP40, 2min at RT each, boiled in sample buffer and the immunoprecipitated proteins resolved by SDS-PAGE in a 10% acrylamide gel (Nupage Invitrogen). Western blotting with anti-Smad4 (SantaCruz B8), anti-beta-catenin

(SIGMA) and anti-Ubiquitin (FK2 Biomol) was done according to (Cordenonsi et al., 2007). Secondary antibody for the detection of Smad4 in anti-Ub immunoprecipitates was ExactaCruz E HRP conjugate.

REFERENCES

Adorno, M., Cordenonsi, M., Montagner, M., Dupont, S., Wong, C., Hann, B., Solari, A., Bobisse, S., Rondina, M.B., Guzzardo, V*., et al.* (2009). A Mutant-p53/Smad complex opposes p63 to empower TGFbeta-induced metastasis. Cell *137*, 87-98.

Amerik, A.Y., and Hochstrasser, M. (2004). Mechanism and function of deubiquitinating enzymes. Biochimica et biophysica acta *1695*, 189-207.

Ang, S.L., and Constam, D.B. (2004). A gene network establishing polarity in the early mouse embryo. Seminars in cell & developmental biology *15*, 555-561.

Anson-Cartwright, L., Dawson, K., Holmyard, D., Fisher, S.J., Lazzarini, R.A., and Cross, J.C. (2000). The glial cells missing-1 protein is essential for branching morphogenesis in the chorioallantoic placenta. Nat Genet *25*, 311-314.

Arnold, S.J., and Robertson, E.J. (2009). Making a commitment: cell lineage allocation and axis patterning in the early mouse embryo. Nature reviews *10*, 91-103.

Bachiller, D., Klingensmith, J., Kemp, C., Belo, J.A., Anderson, R.M., May, S.R., McMahon, J.A., McMahon, A.P., Harland, R.M., Rossant, J*., et al.* (2000). The organizer factors Chordin and Noggin are required for mouse forebrain development. Nature *403*, 658-661.

Bardeesy, N., Cheng, K.H., Berger, J.H., Chu, G.C., Pahler, J., Olson, P., Hezel, A.F., Horner, J., Lauwers, G.Y., Hanahan, D*., et al.* (2006). Smad4 is dispensable for normal pancreas development yet critical in progression and tumor biology of pancreas cancer. Genes Dev *20*, 3130-3146.

Ben-Haim, N., Lu, C., Guzman-Ayala, M., Pescatore, L., Mesnard, D., Bischofberger, M., Naef, F., Robertson, E.J., and Constam, D.B. (2006). The nodal precursor acting via activin receptors induces mesoderm by maintaining a source of its convertases and BMP4. Dev Cell *11*, 313-323.

Brennan, J., Lu, C.C., Norris, D.P., Rodriguez, T.A., Beddington, R.S., and Robertson, E.J. (2001). Nodal signalling in the epiblast patterns the early mouse embryo. Nature *411*, 965-969.

Cammas, F., Garnier, J., Chambon, P., and Losson, R. (2000). Correlation of the exon/intron organization to the conserved domains of the mouse transcriptional corepressor TIF1beta. Gene *253*, 231-235.

Camus, A., Perea-Gomez, A., Moreau, A., and Collignon, J. (2006). Absence of Nodal signaling promotes precocious neural differentiation in the mouse embryo. Dev Biol *295*, 743-755.

Chu, G.C., Dunn, N.R., Anderson, D.C., Oxburgh, L., and Robertson, E.J. (2004). Differential requirements for Smad4 in TGFbeta-dependent patterning of the early mouse embryo. Development *131*, 3501-3512.

Collignon, J., Varlet, I., and Robertson, E.J. (1996). Relationship between asymmetric nodal expression and the direction of embryonic turning. Nature *381*, 155-158.

Constam, D.B., and Robertson, E.J. (2000). SPC4/PACE4 regulates a TGFbeta signaling network during axis formation. Genes Dev *14*, 1146-1155.

Cordenonsi, M., Montagner, M., Adorno, M., Zacchigna, L., Martello, G., Mamidi, A., Soligo, S., Dupont, S., and Piccolo, S. (2007). Integration of TGF-beta and Ras/MAPK signaling through p53 phosphorylation. Science *315*, 840-843.

Derynck, R., Akhurst, R.J., and Balmain, A. (2001). TGF-beta signaling in tumor suppression and cancer progression. Nat Genet *29*, 117-129.

Di-Gregorio, A., Sancho, M., Stuckey, D.W., Crompton, L.A., Godwin, J., Mishina, Y., and Rodriguez, T.A. (2007). BMP signalling inhibits premature neural differentiation in the mouse embryo. Development *134*, 3359-3369.

Ding, J., Yang, L., Yan, Y.T., Chen, A., Desai, N., Wynshaw-Boris, A., and Shen, M.M. (1998). Cripto is required for correct orientation of the anterior-posterior axis in the mouse embryo. Nature *395*, 702-707.

Dunn, N.R., Koonce, C.H., Anderson, D.C., Islam, A., Bikoff, E.K., and Robertson, E.J. (2005). Mice exclusively expressing the short isoform of Smad2 develop normally and are viable and fertile. Genes Dev *19*, 152-163.

Dunn, N.R., Vincent, S.D., Oxburgh, L., Robertson, E.J., and Bikoff, E.K. (2004). Combinatorial activities of Smad2 and Smad3 regulate mesoderm formation and patterning in the mouse embryo. Development *131*, 1717-1728.

Dupe, V., Davenne, M., Brocard, J., Dolle, P., Mark, M., Dierich, A., Chambon, P., and Rijli, F.M. (1997). In vivo functional analysis of the Hoxa-1 3' retinoic acid response element (3'RARE). Development *124*, 399-410.

Dupont, S., Mamidi, A., Cordenonsi, M., Montagner, M., Zacchigna, L., Adorno, M., Martello, G., Stinchfield, M.J., Soligo, S., Morsut, L*., et al.* (2009). FAM/USP9x, a deubiquitinating enzyme essential for TGFbeta signaling, controls Smad4 monoubiquitination. Cell *136*, 123-135.

Dupont, S., Zacchigna, L., Cordenonsi, M., Soligo, S., Adorno, M., Rugge, M., and Piccolo, S. (2005). Germ-layer specification and control of cell growth by Ectodermin, a Smad4 ubiquitin ligase. Cell *121*, 87-99.

Guillemot, F., Caspary, T., Tilghman, S.M., Copeland, N.G., Gilbert, D.J., Jenkins, N.A., Anderson, D.J., Joyner, A.L., Rossant, J., and Nagy, A. (1995). Genomic imprinting of Mash2, a mouse gene required for trophoblast development. Nat Genet *9*, 235-242.

Guzman-Ayala, M., Ben-Haim, N., Beck, S., and Constam, D.B. (2004). Nodal protein processing and fibroblast growth factor 4 synergize to maintain a trophoblast stem cell microenvironment. Proc Natl Acad Sci U S A *101*, 15656-15660.

Hayashi, S., Lewis, P., Pevny, L., and McMahon, A.P. (2002). Efficient gene modulation in mouse epiblast using a Sox2Cre transgenic mouse strain. Gene Expr Patterns *2*, 93-97.

Itoh, S., and ten Dijke, P. (2007). Negative regulation of TGF-beta receptor/Smad signal transduction. Current opinion in cell biology *19*, 176-184.

Izzi, L., and Attisano, L. (2006). Ubiquitin-dependent regulation of TGFbeta signaling in cancer. Neoplasia (New York, NY *8*, 677-688.

Kimura, C., Shen, M.M., Takeda, N., Aizawa, S., and Matsuo, I. (2001). Complementary functions of Otx2 and Cripto in initial patterning of mouse epiblast. Dev Biol *235*, 12-32.

Lin, T.P., Labosky, P.A., Grabel, L.B., Kozak, C.A., Pitman, J.L., Kleeman, J., and MacLeod, C.L. (1994). The Pem homeobox gene is X-linked and exclusively expressed in extraembryonic tissues during early murine development. Dev Biol *166*, 170-179.

Lin, X., Duan, X., Liang, Y.Y., Su, Y., Wrighton, K.H., Long, J., Hu, M., Davis, C.M., Wang, J., Brunicardi, F.C*., et al.* (2006). PPM1A functions as a Smad phosphatase to terminate TGFbeta signaling. Cell *125*, 915-928.

Lowe, L.A., Yamada, S., and Kuehn, M.R. (2001). Genetic dissection of nodal function in patterning the mouse embryo. Development *128*, 1831-1843.

Lu, C.C., and Robertson, E.J. (2004). Multiple roles for Nodal in the epiblast of the mouse embryo in the establishment of anterior-posterior patterning. Dev Biol *273*, 149-159.

Massague, J. (2000). How cells read TGF-beta signals. Nature reviews *1*, 169-178.

Mesnard, D., Guzman-Ayala, M., and Constam, D.B. (2006). Nodal specifies embryonic visceral endoderm and sustains pluripotent cells in the epiblast before overt axial patterning. Development *133*, 2497-2505.

Moffat, J., Grueneberg, D.A., Yang, X., Kim, S.Y., Kloepfer, A.M., Hinkle, G., Piqani, B., Eisenhaure, T.M., Luo, B., Grenier, J.K*., et al.* (2006). A lentiviral RNAi library for human and mouse genes applied to an arrayed viral high-content screen. Cell *124*, 1283-1298.

Moren, A., Imamura, T., Miyazono, K., Heldin, C.H., and Moustakas, A. (2005). Degradation of the tumor suppressor Smad4 by WW and HECT domain ubiquitin ligases. J Biol Chem *280*, 22115-22123.

Narimatsu, M., Bose, R., Pye, M., Zhang, L., Miller, B., Ching, P., Sakuma, R., Luga, V., Roncari, L., Attisano, L.*, et al.* (2009). Regulation of planar cell polarity by Smurf ubiquitin ligases. Cell *137*, 295-307.

Nijman, S.M., Luna-Vargas, M.P., Velds, A., Brummelkamp, T.R., Dirac, A.M., Sixma, T.K., and Bernards, R. (2005). A genomic and functional inventory of deubiquitinating enzymes. Cell *123*, 773-786.

Norris, D.P., Brennan, J., Bikoff, E.K., and Robertson, E.J. (2002). The Foxh1-dependent autoregulatory enhancer controls the level of Nodal signals in the mouse embryo. Development *129*, 3455-3468.

Perea-Gomez, A., Vella, F.D., Shawlot, W., Oulad-Abdelghani, M., Chazaud, C., Meno, C., Pfister, V., Chen, L., Robertson, E., Hamada, H.*, et al.* (2002). Nodal antagonists in the anterior visceral endoderm prevent the formation of multiple primitive streaks. Dev Cell *3*, 745-756.

Pfister, S., Steiner, K.A., and Tam, P.P. (2007). Gene expression pattern and progression of embryogenesis in the immediate post-implantation period of mouse development. Gene Expr Patterns *7*, 558-573.

Piccolo, S., Agius, E., Leyns, L., Bhattacharyya, S., Grunz, H., Bouwmeester, T., and De Robertis, E.M. (1999). The head inducer Cerberus is a multifunctional antagonist of Nodal, BMP and Wnt signals. Nature *397*, 707-710.

Pickart, C.M. (2001). Mechanisms underlying ubiquitination. Annual review of biochemistry *70*, 503-533.

Rodriguez, R.T., Velkey, J.M., Lutzko, C., Seerke, R., Kohn, D.B., O'Shea, K.S., and Firpo, M.T. (2007). Manipulation of OCT4 levels in human embryonic stem cells results in induction of differential cell types. Experimental biology and medicine (Maywood, NJ *232*, 1368-1380.

Rodriguez, T.A., Srinivas, S., Clements, M.P., Smith, J.C., and Beddington, R.S. (2005). Induction and migration of the anterior visceral endoderm is regulated by the extra-embryonic ectoderm. Development *132*, 2513-2520.

Sakai, K., and Miyazaki, J. (1997). A transgenic mouse line that retains Cre recombinase activity in mature oocytes irrespective of the cre transgene transmission. Biochem Biophys Res Commun *237*, 318-324.

Salmena, L., and Pandolfi, P.P. (2007). Changing venues for tumour suppression: balancing destruction and localization by monoubiquitylation. Nat Rev Cancer *7*, 409-413.

Schmierer, B., and Hill, C.S. (2005). Kinetic analysis of Smad nucleocytoplasmic shuttling reveals a mechanism for transforming growth factor beta-dependent nuclear accumulation of Smads. Molecular and cellular biology *25*, 9845-9858.

Sirard, C., de la Pompa, J.L., Elia, A., Itie, A., Mirtsos, C., Cheung, A., Hahn, S., Wakeham, A., Schwartz, L., Kern, S.E.*, et al.* (1998). The tumor suppressor gene Smad4/Dpc4 is required for gastrulation and later for anterior development of the mouse embryo. Genes Dev *12*, 107-119.

Sulik, K., Dehart, D.B., Iangaki, T., Carson, J.L., Vrablic, T., Gesteland, K., and Schoenwolf, G.C. (1994). Morphogenesis of the murine node and notochordal plate. Dev Dyn *201*, 260-278.

Tam, P.P., and Loebel, D.A. (2007). Gene function in mouse embryogenesis: get set for gastrulation. Nat Rev Genet *8*, 368-381.

Tam, P.P., Loebel, D.A., and Tanaka, S.S. (2006). Building the mouse gastrula: signals, asymmetry and lineages. Current opinion in genetics & development *16*, 419-425.

Tanaka, S., Kunath, T., Hadjantonakis, A.K., Nagy, A., and Rossant, J. (1998). Promotion of trophoblast stem cell proliferation by FGF4. Science *282*, 2072-2075.

Tremblay, K.D., Hoodless, P.A., Bikoff, E.K., and Robertson, E.J. (2000). Formation of the definitive endoderm in mouse is a Smad2-dependent process. Development *127*, 3079-3090.

Varlet, I., Collignon, J., and Robertson, E.J. (1997). nodal expression in the primitive endoderm is required for specification of the anterior axis during mouse gastrulation. Development *124*, 1033-1044.

Vincent, S.D., Dunn, N.R., Hayashi, S., Norris, D.P., and Robertson, E.J. (2003). Cell fate decisions within the mouse organizer are governed by graded Nodal signals. Genes Dev *17*, 1646-1662.

Wakefield, L.M., and Roberts, A.B. (2002). TGF-beta signaling: positive and negative effects on tumorigenesis. Current opinion in genetics & development *12*, 22-29.

Waldrip, W.R., Bikoff, E.K., Hoodless, P.A., Wrana, J.L., and Robertson, E.J. (1998). Smad2 signaling in extraembryonic tissues determines anterior-posterior polarity of the early mouse embryo. Cell *92*, 797-808.

Wood, S.A., Pascoe, W.S., Ru, K., Yamada, T., Hirchenhain, J., Kemler, R., and Mattick, J.S. (1997). Cloning and expression analysis of a novel mouse gene with sequence similarity to the Drosophila fat facets gene. Mech Dev *63*, 29-38.

Wrana, J.L. (2009). The secret life of Smad4. Cell *136*, 13-14.

Yamamoto, M., Beppu, H., Takaoka, K., Meno, C., Li, E., Miyazono, K., and Hamada, H. (2009). Antagonism between Smad1 and Smad2 signaling determines the site of distal visceral endoderm formation in the mouse embryo. J Cell Biol *184*, 323-334.

Yan, K.P., Dolle, P., Mark, M., Lerouge, T., Wendling, O., Chambon, P., and Losson, R. (2004). Molecular cloning, genomic structure, and expression analysis of the mouse transcriptional intermediary factor 1 gamma gene. Gene *334*, 3-13.

Yang, X., Li, C., Xu, X., and Deng, C. (1998). The tumor suppressor SMAD4/DPC4 is essential for epiblast proliferation and mesoderm induction in mice. Proc Natl Acad Sci U S A *95*, 3667-3672.

Zhu, H., Kavsak, P., Abdollah, S., Wrana, J.L., and Thomsen, G.H. (1999). A SMAD ubiquitin ligase targets the BMP pathway and affects embryonic pattern formation. Nature *400*, 687-693.

FIGURES

Figure 1. Early mouse embryonic development.

a) 4.0 days after fertilization (stage E4.0) the mouse embryo is ready for implantation in the uterine wall; the embryo is composed by three differentiated lineages, namely trophectoderm (grey), primitive endoderm (yellow) and inner cell mass (light blue).

b,c) At around E5.5 the egg cylinder has formed, thanks to the elongation of the blastocyst; this originates the proximo-distal (P-D) axis. The epiblast has undergone cavitation, originating the proamniotic cavity.

d,e) At around E6.5 gastrulation starts: at a discrete place in the proximal epiblast, mesoderm is induced. The primitive streak begins the elongation towards the distal tip of the egg cylinder: this elongation originates the first axis of the embryo proper, the antero-posterior (Ant-Post) axis.

Modified from Tam and Loebel, 2007.

FIGURE 1

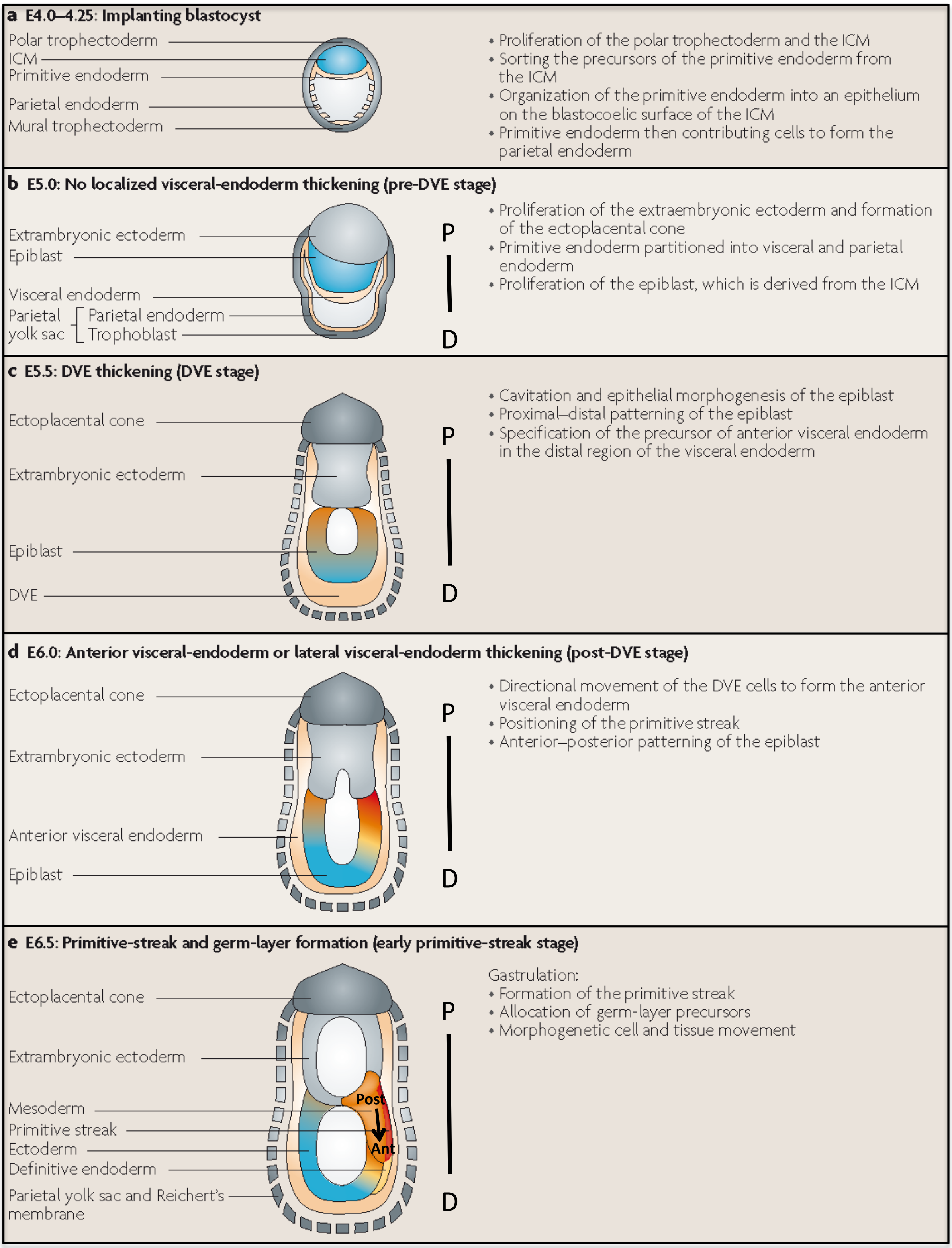

a **E4.0–4.25: Implanting blastocyst**

Polar trophectoderm
ICM
Primitive endoderm
Parietal endoderm
Mural trophectoderm

- Proliferation of the polar trophectoderm and the ICM
- Sorting the precursors of the primitive endoderm from the ICM
- Organization of the primitive endoderm into an epithelium on the blastocoelic surface of the ICM
- Primitive endoderm then contributing cells to form the parietal endoderm

b **E5.0: No localized visceral-endoderm thickening (pre-DVE stage)**

Extrambryonic ectoderm
Epiblast
Visceral endoderm
Parietal yolk sac
Parietal endoderm
Trophoblast
P
D

- Proliferation of the extraembryonic ectoderm and formation of the ectoplacental cone
- Primitive endoderm partitioned into visceral and parietal endoderm
- Proliferation of the epiblast, which is derived from the ICM

c **E5.5: DVE thickening (DVE stage)**

Ectoplacental cone
Extrambryonic ectoderm
Epiblast
DVE
P
D

- Cavitation and epithelial morphogenesis of the epiblast
- Proximal–distal patterning of the epiblast
- Specification of the precursor of anterior visceral endoderm in the distal region of the visceral endoderm

d **E6.0: Anterior visceral-endoderm or lateral visceral-endoderm thickening (post-DVE stage)**

Ectoplacental cone
Extrambryonic ectoderm
Anterior visceral endoderm
Epiblast
P
D

- Directional movement of the DVE cells to form the anterior visceral endoderm
- Positioning of the primitive streak
- Anterior–posterior patterning of the epiblast

e **E6.5: Primitive-streak and germ-layer formation (early primitive-streak stage)**

Ectoplacental cone
Extrambryonic ectoderm
Mesoderm
Primitive streak
Ectoderm
Definitive endoderm
Parietal yolk sac and Reichert's membrane
Post
Ant
P
D

Gastrulation:
- Formation of the primitive streak
- Allocation of germ-layer precursors
- Morphogenetic cell and tissue movement

Figure 2. The organizer/Node of the mouse embryo.

a) Mesoderm induction converts a group of epiblast cells to mesenchimal fate. These cells migrate between epiblast and visceral endoderm, giving rise to the trilaminar embryo. The movement of epiblast cells beneath this epithelial sheet originates the primitive streak, and contributes to the elongation of the embryo during gastrulation. Embryos are shown from the side, anterior to the left. Modified from Arnold and Robertson, 2009.

b) When the primitive streak reaches the distal tip of the egg cylinder, the cells of this region self aggregate in a bilaminar structure known as the Node (light blue). This group of cells has organizing properties, and orchestrates the deposition of mesoderm, endoderm and neurectoderm during the subsequent stages of development (Arnold and Robertson, 2009).

c) An electronic microscopy image showing the inside of a mouse embryo, at around E7.5. Arrow points to the allantois. On the distal part the Node (N) and the Anterior Mesendoderm (AME) are recognizable. Modified from Sulik et al., 1994.

d) Looking at an intact Node from the point of view shown in **c**, the structural organization of the outside layer of the Node and of the anterior mesendoderm is visible. en, definitive endoderm. Arrow points to the node. Modified from Sulik et al., 1994.

FIGURE 2

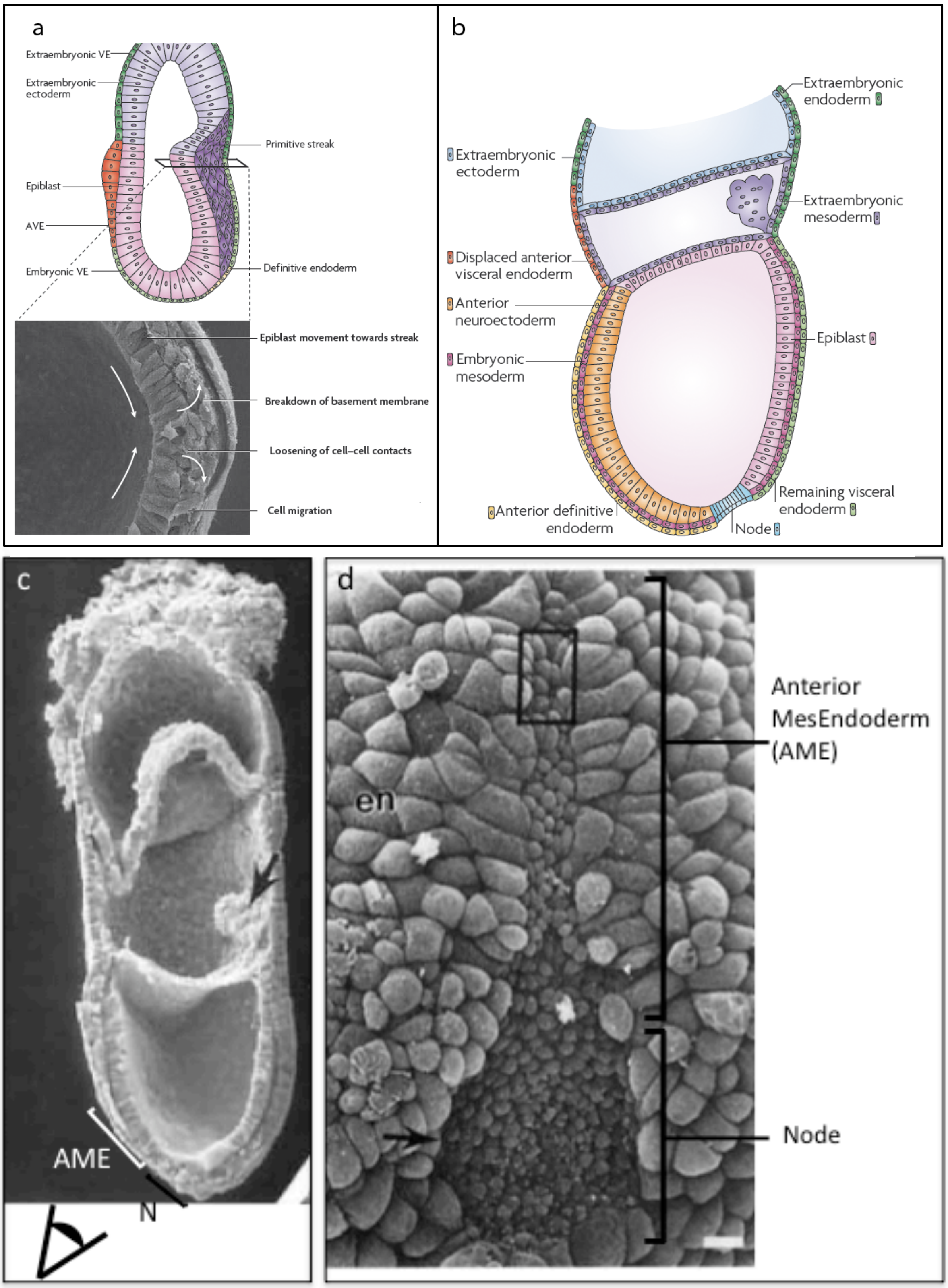
a
Extraembryonic VE
Extraembryonic ectoderm
Primitive streak
Epiblast
AVE
Embryonic VE
Definitive endoderm
Epiblast movement towards streak
Breakdown of basement membrane
Loosening of cell–cell contacts
Cell migration
b
Extraembryonic endoderm
Extraembryonic ectoderm
Extraembryonic mesoderm
Displaced anterior visceral endoderm
Anterior neuroectoderm
Epiblast
Embryonic mesoderm
Remaining visceral endoderm
Anterior definitive endoderm
Node
c
AME
N
d
en
Anterior MesEndoderm (AME)
Node

Figure 3. The Transforming Growth Factor-β (TGFβ) signal transduction pathway.

a) The TGFβ cascade. TGFβ ligands bind the serine-threonine kinase receptors on the cell surface; this event activate the receptors that in turn phosphorylate and thus activate receptor Smads (R-Smads), which are the first intracellular signal mediators. The R-Smads bind Smad-4, the Co-Smad, and this multimer translocates into the nucleus; here, specific target genes transcription will be regulated (Massague, 2000).

b) The proposed cycle of monoubiquitination/deubiquitination of Smad4. The two enzymes involved, Ectodermin/Tif1γ/TRIM33 and FAM/Usp9x trigger the opposing reactions, respectively in the nucleus and in the cytoplasm. This cycle allows the cells to maintain a reliably transduction of rapidly varying signals from the extracellular space (Wrana, 2009).

FIGURE 3

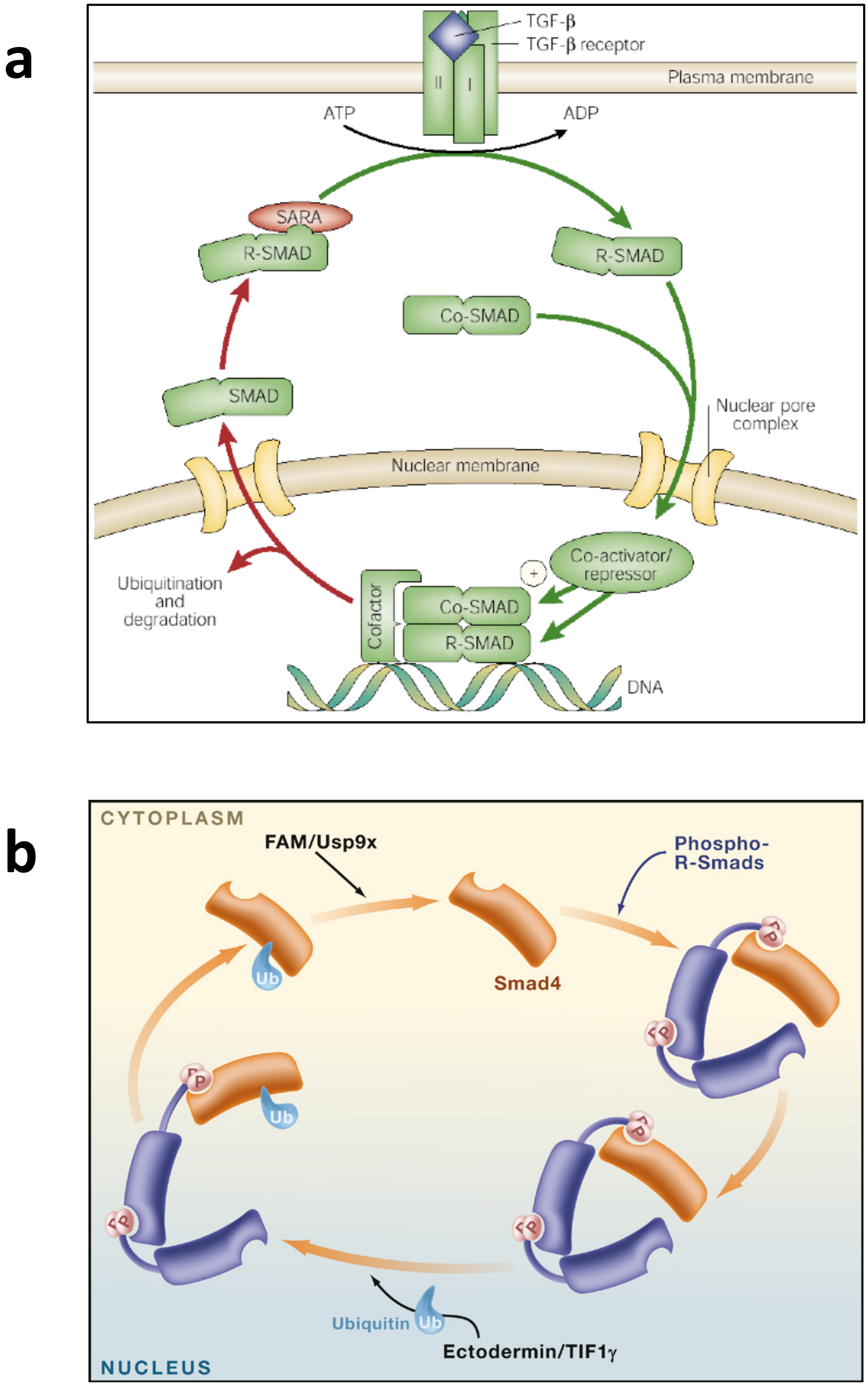
a
TGF-β
TGF-β receptor
Plasma membrane
II
I
ATP
ADP
SARA
R-SMAD
R-SMAD
Co-SMAD
SMAD
Nuclear pore complex
Nuclear membrane
Ubiquitination and degradation
Co-activator/ repressor
+
Cofactor
Co-SMAD
R-SMAD
DNA
b
CYTOPLASM
FAM/Usp9x
Phospho-R-Smads
Ub
Smad4
P
Ub
Ubiquitin
Ectodermin/TIF1γ
NUCLEUS

Figure 4. Major TGFβ roles during early mouse development.

a) Events that requires Nodal during early mouse development. The principal TGFβ ligand of the early mouse embryo is Nodal; by E5.0 it is expressed widely in the epiblast (violet) and in the surrounding visceral endoderm (not shown in this scheme for clarity reasons).

At E5.5, Nodal gives positive signal both to the distal visceral endoderm, where the AVE (red) is induced, and to the trophoblast, where the trophoblast stem cells (TS, yellow) start growing and differentiating.

At E6.5 mouse gastrulation begins; AVE rotates towards the prospective anterior side, and mesoderm induction happens at the opposite pole of the epiblast (light blue). Nodal is a fundamental cue for mesoderm induction; other positive signals come from the trophoblast compartment. Mesoderm induction originates an elongated structure known as primitive streak (PS) that is patterned mainly by a Nodal morphogenetic field (depicted as a gradient from dark blue (anterior PS) to light blue (posterior PS)).

b) Nodal dose dependency for some of the Nodal-dependent phenomena of early mouse development. Thanks to several genetics studies that exploit stepwise reduction of Nodal signaling, a dose dependency is known for at least some Nodal-dependent events: AVE induction, AVE migration and anterior primitive streak (APS) / Node induction are thought to require increasingly high dosage of Nodal signaling. This model is based on knockout studies of agonists of the pathway. In particular, AVE induction is lost in Nodal and Smad2 knockout embryos (nodal-/- and Smad2-/-); AVE rotation is lost in a severe Nodal hypomorph combination (Δ600/-) and in Cripto and FoxH1 single knockouts; APS/Node induction is lost in Smad4 epiblast specific knockouts (Smad4-EpiKO). Modified from Norris et al., 2002.

FIGURE 4

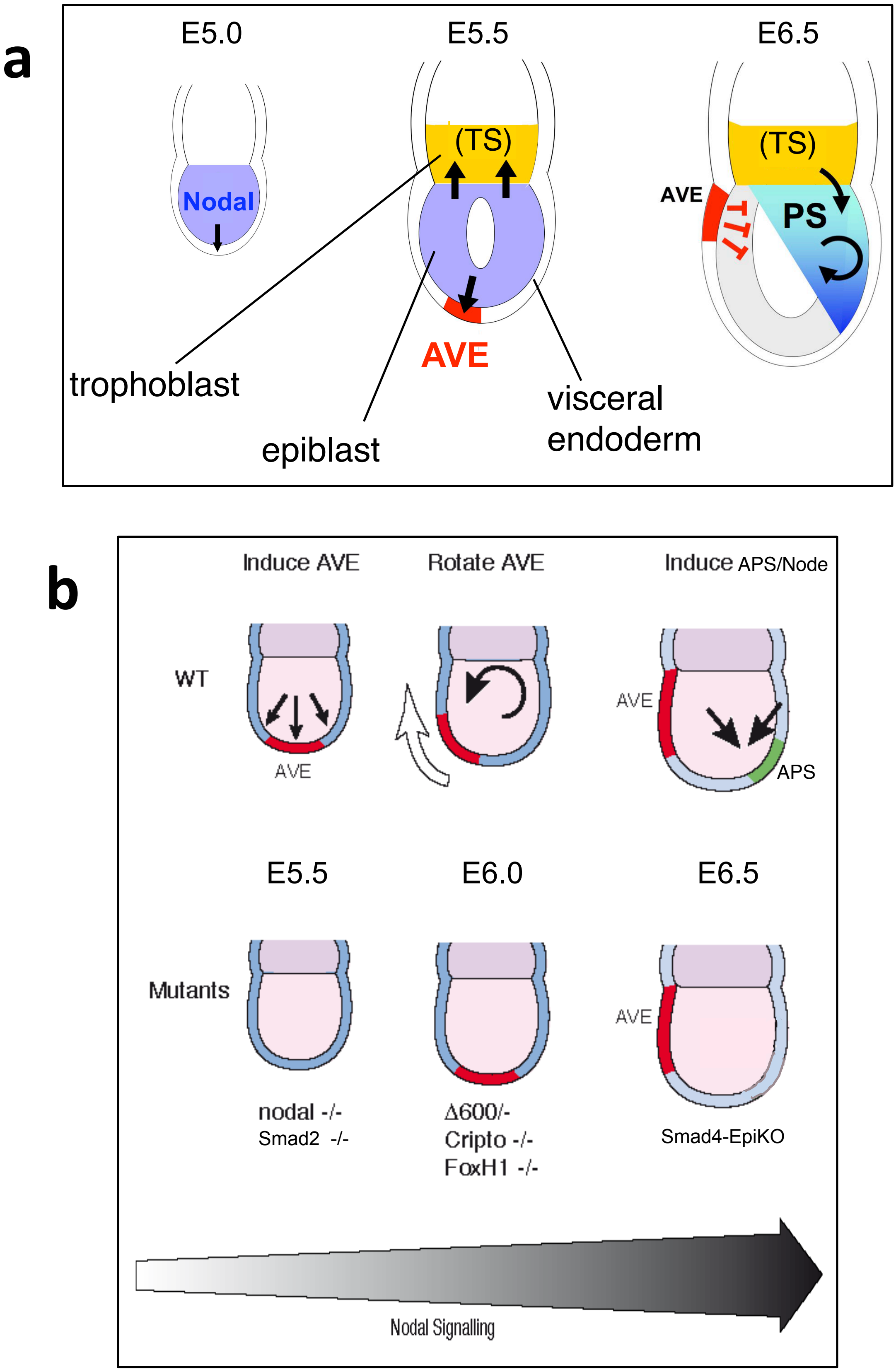
a
E5.0
E5.5
E6.5
Nodal
(TS)
(TS)
AVE
PS
AVE
trophoblast
epiblast
visceral
endoderm
b
Induce AVE
Rotate AVE
Induce APS/Node
WT
AVE
AVE
APS
E5.5
E6.0
E6.5
Mutants
AVE
nodal -/-
Smad2 -/-
Δ600/-
Cripto -/-
FoxH1 -/-
Smad4-EpiKO
Nodal Signalling

Figure 5. Generation of *Ecto* alleles and *Ecto-/-* embryos morphology.

a) Diagram showing a partial map of the genomic locus surrounding exons 2, 3 and 4 of the Ecto/Tif1γ gene, the targeting construct, and the targeted allele before and after Cre-mediated excision of the neomycin-resistance selection marker (PGK-Neo). The 3' probe used for Southern blot analysis and the fragment sizes detected with the 3' probe and the Neo probe upon HindIII and BglI digestion are indicated. Relevant restriction sites: B, BglI; Ba, BamHI; E, EcoRI; H, HindIII; N, NheI; S, SacI; X, XcmI, Xb, XbaI. On the bottom left, schematic representation of wild-type Ecto/Tif1γ protein (WT) and of the predicted mutant protein expressed from the recombined *Ecto* locus. The structural and functional domains are indicated. The putative product of the deleted Ecto/Tif1γ gene corresponds to a C-terminally truncated peptide consisting of the first 191 amino acids of the protein. On the bottom right, southern blot analysis of genomic DNAs derived from wild-type (+/+) and targeted ES cells. Genomic DNA was digested with HindIII or BglI, blotted and hybridized with the 3' probe or the Neo probe.

b) Hematoxilin and Eosin staining of sections of wild-type (WT) and Ecto-/- embryos within intact decidual tissues at early-streak stage. Note the absence of primitive streak formation (arrowhead) and how the embryo lacks a distinction between epiblast (epi.) and extraembryonic ectoderm (EXE). Scale bars correspond to 10μm.

FIGURE 5

a

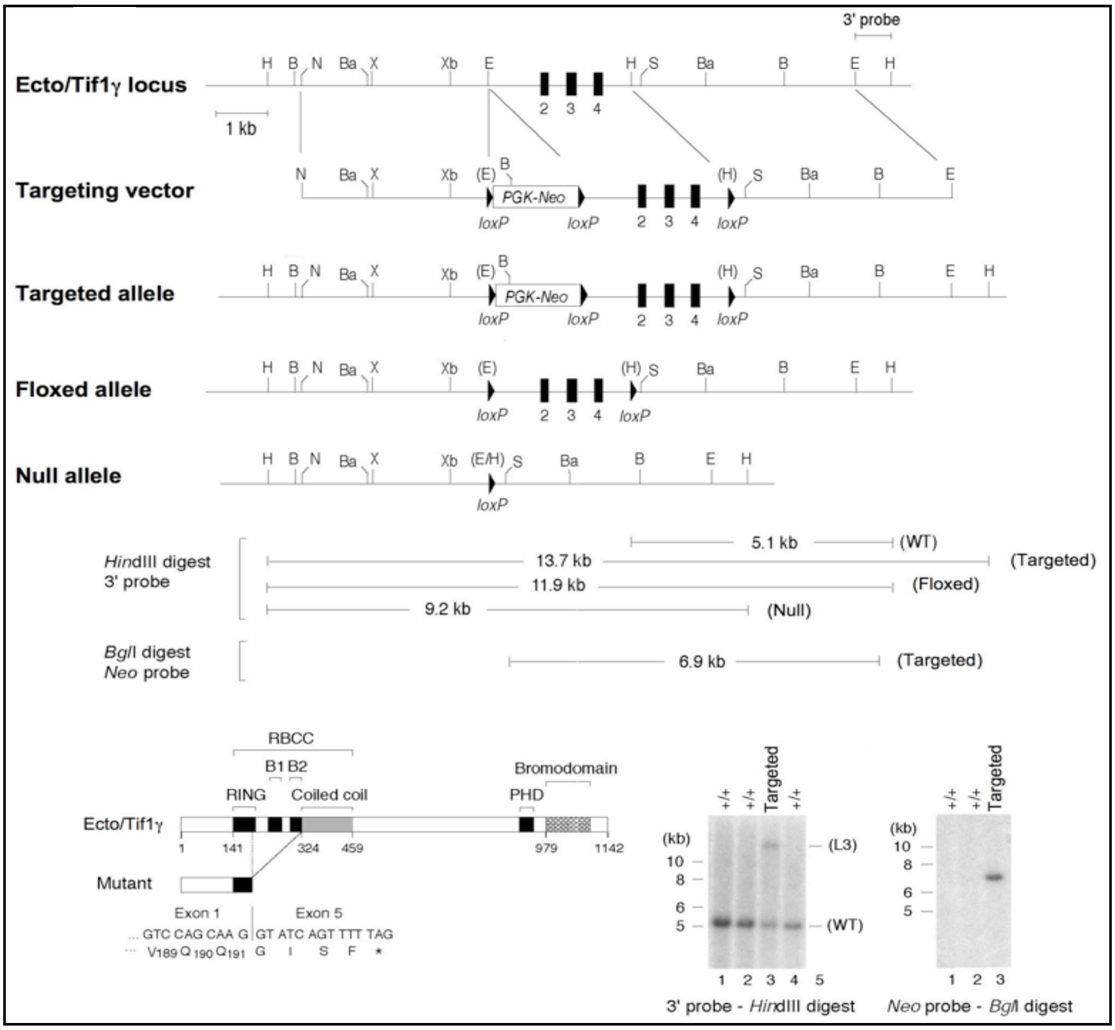
3' probe
Ecto/Tif1γ locus
H B N Ba X Xb E H S Ba B E H
2 3 4
1 kb
Targeting vector
N Ba X Xb (E) B (H) S Ba B E
PGK-Neo
loxP loxP 2 3 4 loxP
Targeted allele
H B N Ba X Xb (E) B (H) S Ba B E H
PGK-Neo
loxP loxP 2 3 4 loxP
Floxed allele
H B N Ba X Xb (E) (H) S Ba B E H
loxP 2 3 4 loxP
Null allele
H B N Ba X Xb (E/H) S Ba B E H
loxP
*Hin*dIII digest
3' probe
5.1 kb (WT)
13.7 kb (Targeted)
11.9 kb (Floxed)
9.2 kb (Null)
*Bgl*I digest
Neo probe
6.9 kb (Targeted)
RBCC
B1 B2
RING
Coiled coil
PHD
Bromodomain
Ecto/Tif1γ
1 141 324 459 979 1142
Mutant
Exon 1
Exon 5
... GTC CAG CAA G GT ATC AGT TTT TAG
··· V189 Q190 Q191 G I S F *
+/+ +/+ Targeted +/+
(kb)
10
8
6
5
(L3)
(WT)
1 2 3 4 5
3' probe - *Hin*dIII digest
+/+ +/+ Targeted
(kb)
10
8
6
5
1 2 3
Neo probe - *Bgl*I digest

b

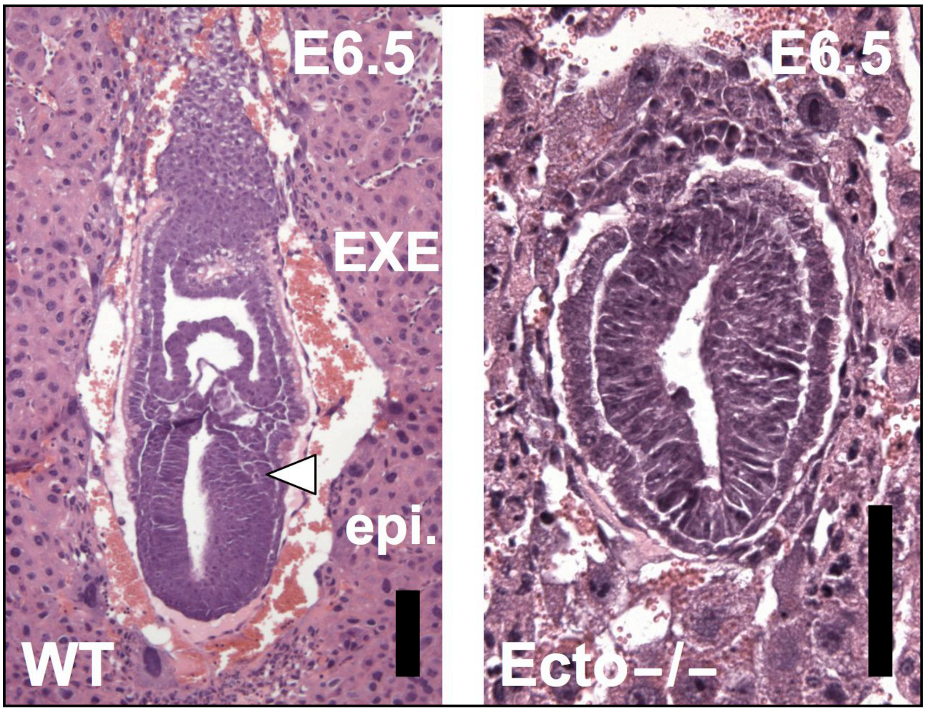
E6.5
EXE
epi.
WT
E6.5
Ecto–/–

Figure 6. Impaired mesoderm master genes induction in *Ecto-/-* embryos.

E6.5 *Ecto* mutant embryos do not express the pan-mesodermal marker *T* (also known as *Brachyury*), the extraembryonic ectoderm and mesoderm marker *Eomes*, and the early mesoderm marker *Wnt3*. Lateral views, anterior to the left.

FIGURE 6

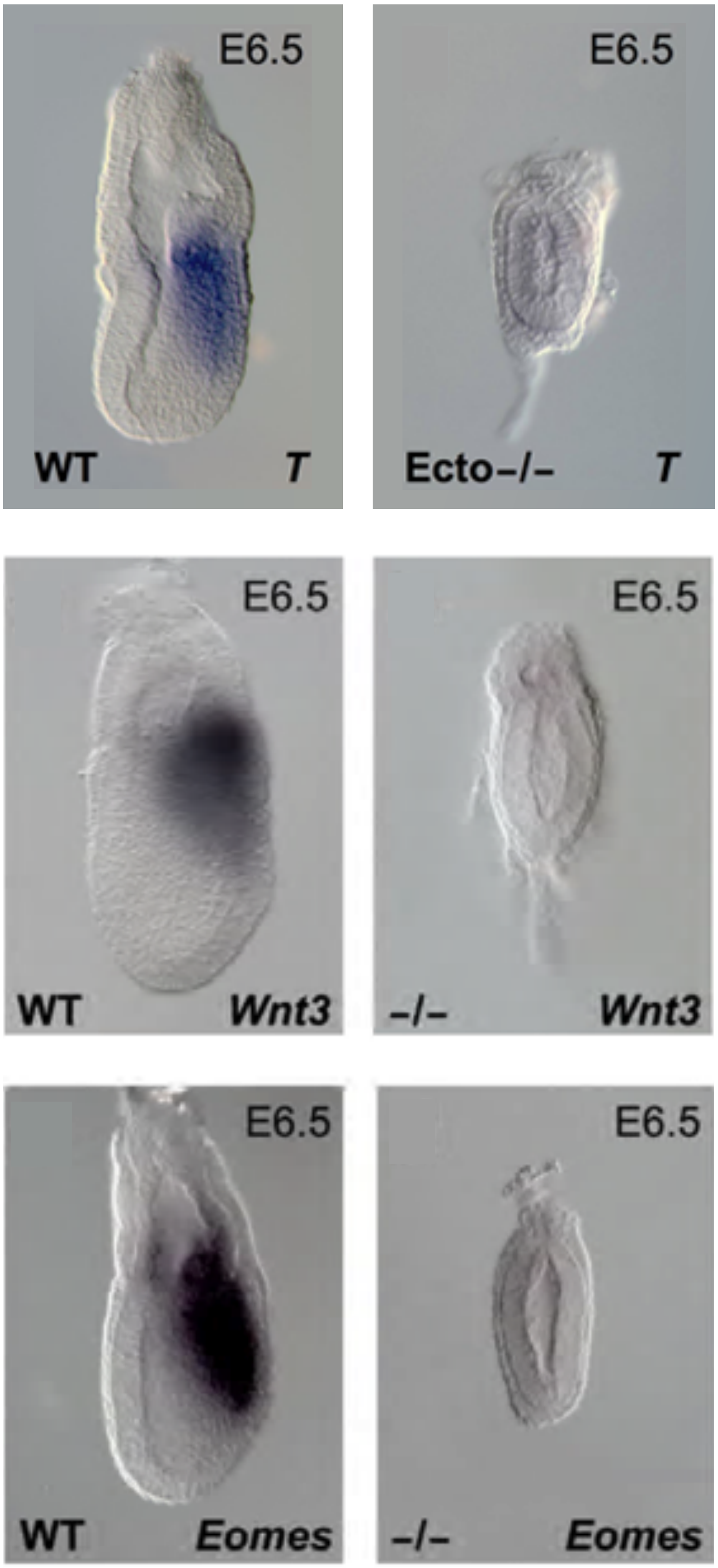
E6.5
WT
T
E6.5
Ecto–/–
T
E6.5
WT
Wnt3
E6.5
–/–
Wnt3
E6.5
WT
Eomes
E6.5
–/–
Eomes

Figure 7. *Ecto* homozygous mutant embryos display abnormally expanded Anterior Visceral Endoderm (AVE).

a) At early pregastrulation stages, AVE is strongly expanded in *Ecto* mutants, as assayed by expression of the Nodal/Smad targets *Cerl* and *Lefty1*.

b) As development proceeds, the AVE of *Ecto*-deficient (-/-) embryos further expands, encircling the epiblast. Lateral views, anterior to the left, of early-streak stage embryos (wild type, WT, and *Ecto* knockout, -/-) stained for *Cerl* and *Lim1* are shown in the upper part of the panel. Transverse (or optical) sections of early-streak stage embryos stained for the same markers are provided in the bottom part (anterior to the left).

Note on the right part that while in wild-type embryos *Lim1* stains both the AVE and the posterior primitive streak, in *Ecto* mutants the AVE is much broader and the mesodermal expression domain of *Lim1* is lost.

c) A schematic representation of the model. The earliest *Nodal*-dependent phenomenon of mouse embryogenesis, AVE induction, is much exaggerated in *Ecto-/-* (-/-) embryos.

FIGURE 7

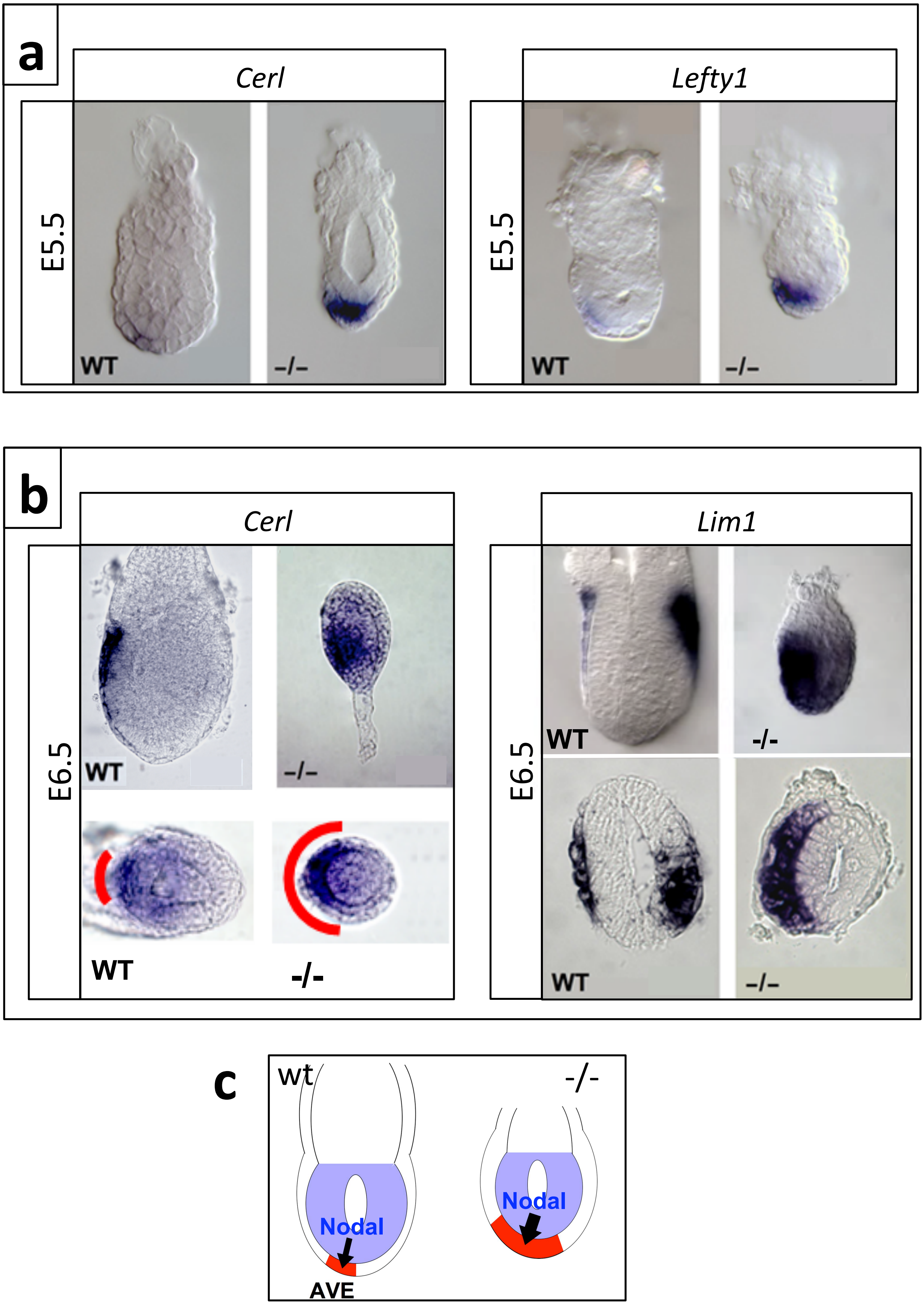
a
Cerl
Lefty1
E5.5
WT
–/–
E5.5
WT
–/–
b
Cerl
Lim1
E6.5
WT
–/–
WT
-/-
E6.5
WT
-/-
WT
–/–
c
wt
-/-
Nodal
AVE
Nodal

Figure 8. *Ecto* acts cell-autonomously within the extraembryonic tissues to restrain AVE formation.

a) Panels show in situ for *Cerl* at pre-streak stage in wild-type and *Sox2Cre;Ecto fl/- (EpiKO)* embryos, namely, in embryos where *Ecto* is inactivated in epiblast cells, but not in extraembryonic tissues.

b) *Nodal* is normally expressed in *Ecto* mutants at E5.5, but it is rapidly downregulated as development proceeds.

c) Smad2 is normally activated in *Ecto* mutants, as assayed by immunofluorescence for phospho-Smad2 (P-Sm2, red channel). Merged images with nuclear counterstain are also shown (YOYO1, green channel).

FIGURE 8

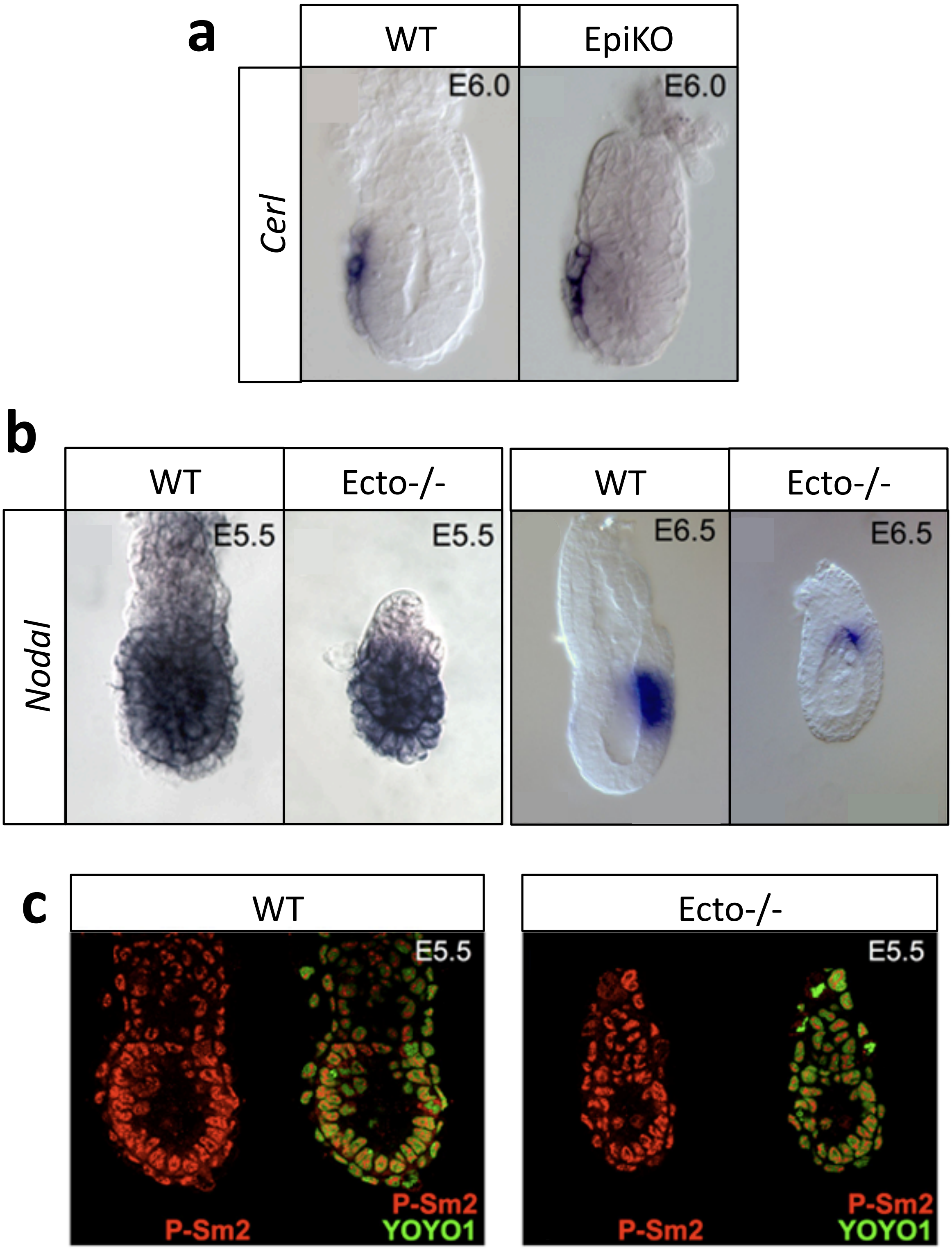
a
WT
EpiKO
E6.0
E6.0
Cerl
b
WT
Ecto-/-
WT
Ecto-/-
E5.5
E5.5
E6.5
E6.5
Nodal
c
WT
Ecto-/-
E5.5
P-Sm2
P-Sm2
YOYO1
E5.5
P-Sm2
P-Sm2
YOYO1

Figure 9. Defective AVE patterning in *Ecto* mutants is mediated by Smad4.

a) Excessive AVE formation in *Ecto* mutants is dependent on Smad4 activity. In situ hybridization for the AVE markers *Cerl* and *Lim1* in wild-type (WT), *Ecto-/-*, *Smad4-/-* and *Ecto/Smad4* double mutant (*Ecto*-/- *Smad4*-/-) embryos. AVE expansion is observed in *Ecto* mutants but not in embryos also lacking *Smad4*.

b) Visceral Endoderm (VE) specification occurs normally in *Smad4-/-* embryos. In situ hybridization for the visceral endoderm (VE) marker alpha-feto protein (*AFP*) on E6.0 wild-type (WT) and *Smad4-/-* embryos. *AFP* staining in *Smad4* deficient embryos serves as control that the visceral endoderm is correctly specified even if it cannot be induced to AVE in the presence or absence of *Ecto*.

FIGURE 9

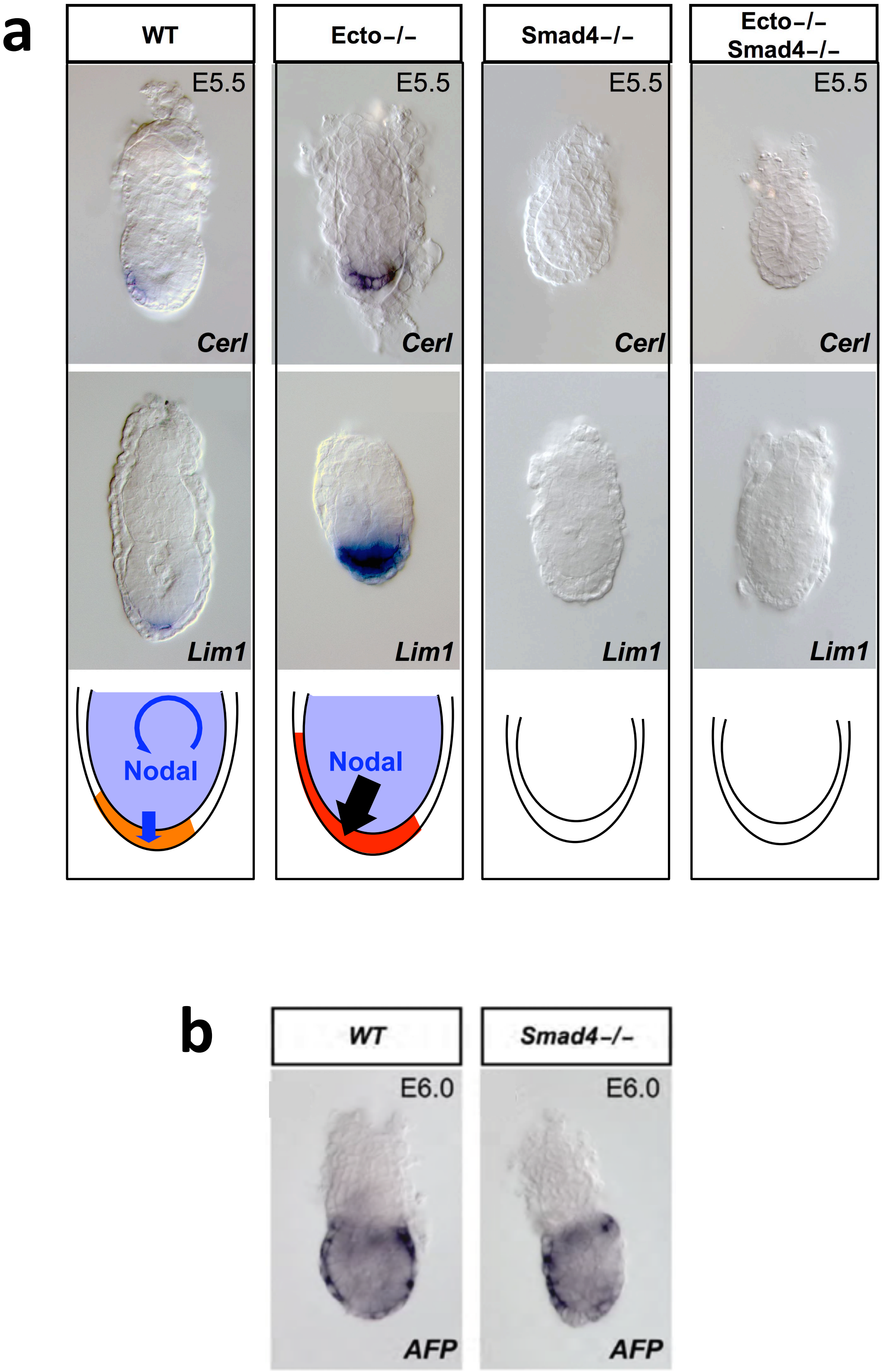
a
WT
Ecto-/-
Smad4-/-
Ecto-/-
Smad4-/-
E5.5
Cerl
Lim1
Nodal
b
WT
Smad4-/-
E6.0
AFP

Figure 10. Reduction of Nodal signaling counterbalances AVE expansion in *Ecto* mutants.

a) Reduction of Nodal signaling by the combined use of null (*Nodal-*) and hypomorphic (*NodalΔ600*) alleles neutralize AVE expansion in *Ecto* mutants, as assayed by in situ hybridization for *Lim1* at pre-streak stage. Note how decreased *Nodal* also rescues the overall morphology and size of the *Ecto* mutants. Lateral views, anterior to the left.

b) Nodal signaling can be deconvoluted into two components: ligand availability (light blue) and intracellular responsiveness, i.e. Smad activity (red). Enhancing responsiveness as in *Ecto-/-* embryos can surpass the threshold for normal AVE induction, but this can be normalized by reducing ligand availability.

c) *Lim1* in situ hybridization at early streak stage in wild-type (WT), *NodalΔ600*/- and compound *NodalΔ600*/-;*Ecto*-/- embryos. Note how reduction of Nodal signaling in *NodalΔ600*/- embryos impairs rotation of the AVE (white arrowhead) toward the anterior pole of the embryo, and how this rotation is restored by inactivation of *Ecto* in *NodalΔ600*/-; *Ecto*-/- embryos. Lateral view, anterior to the left.

FIGURE 10

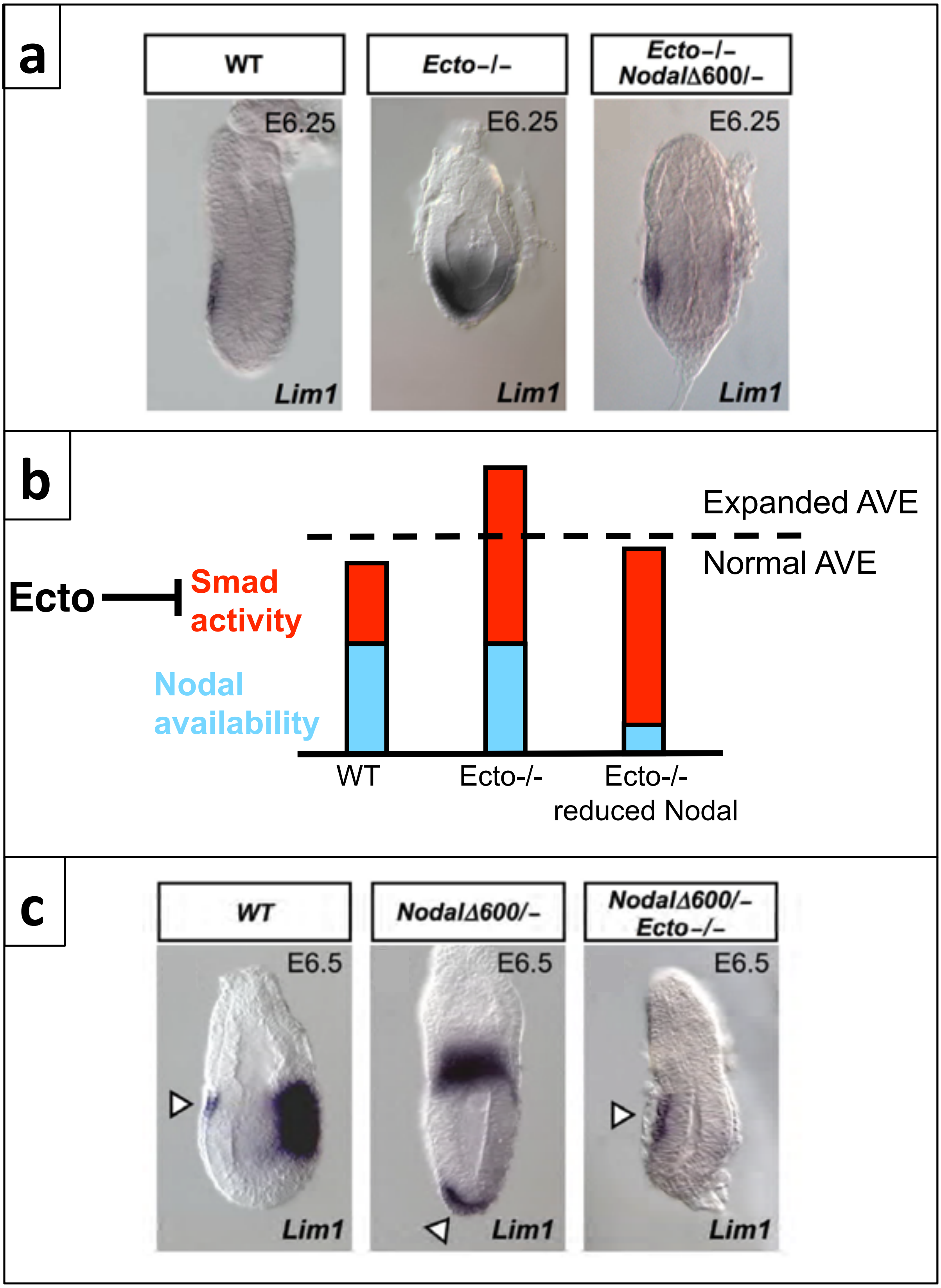
a
WT
Ecto–/–
Ecto–/–
NodalΔ600/–
E6.25
E6.25
E6.25
Lim1
Lim1
Lim1
b
Ecto
Smad activity
Nodal availability
Expanded AVE
Normal AVE
WT
Ecto-/-
Ecto-/-
reduced Nodal
c
WT
NodalΔ600/–
NodalΔ600/–
Ecto–/–
E6.5
E6.5
E6.5
Lim1
Lim1
Lim1

Figure 11. *Ecto* maintains EXE self-renewal by opposing Nodal signaling.

a) *Ecto* mutants (Ecto-/-) lack expression of trophoblast stem (TS) cell markers *Eomes*, *Cdx2* and *BMP4* at E5.5.

b) The epiblast markers *FGF4* and *Oct4* are normally expressed in *Ecto* mutants (Ecto-/-).

c) *Ecto* acts cell-autonomously within the extraembryonic tissues to maintain EXE fates. Panels show in situ for *BMP4* in wild-type and *Sox2-Cre;Ecto fl/- (EpiKO*) embryos, namely, in embryos where *Ecto* is inactivated in epiblast cells, but not in extraembryonic tissues.

d) Reduction of *Nodal* dosage rescues EXE formation in *Ecto* mutant embryos, as assayed by *BMP4* expression. Note that EXE compartment is rescued both in the compound mutants *Ecto-/-; Nodal+/-* and *Ecto-/-; NodalΔ600/-*.

FIGURE 11

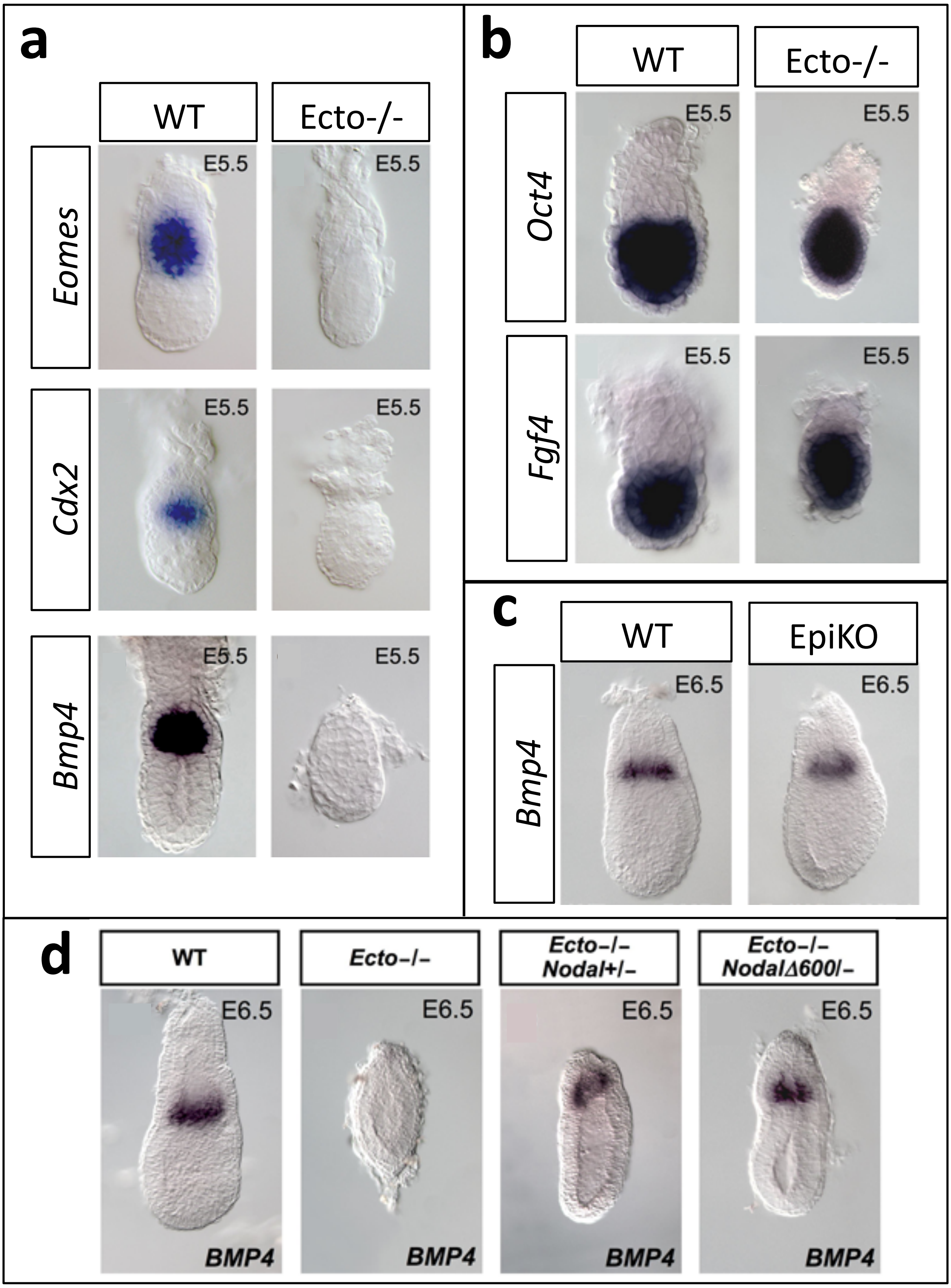
a
WT
Ecto-/-
Eomes
Cdx2
Bmp4
E5.5
b
WT
Ecto-/-
Oct4
Fgf4
E5.5
c
WT
EpiKO
Bmp4
E6.5
d
WT
Ecto–/–
Ecto–/– Nodal+/–
Ecto–/– NodalΔ600/–
E6.5
BMP4

Figure 12. *Ecto* prevents Nodal-induced differentiation of trophoblast stem (TS) cells.

a) The trophoblast lineage is correctly specified in *Ecto* mutants, as assayed by *Cdx2* expression at early post-implantation stages (E4.75). *Ecto* mutants retain *SPC4* and *Pem* expression within the differentiated trophoblast/ectoplacental cone. The trophoblast early differentiation/transient-amplifying marker *Mash2* is lacking in *Ecto* mutants.

b) Immunoblotting for Ecto shows efficient protein depletion in TS cells stably expressing Ecto shRNA (shE). LaminB serves as loading control. * indicates an aspecific band detected by the anti-Ecto antibody.

c) Real-time qPCR analysis of TS cell markers. Control (Co.) and Ecto shRNA-depleted (shE) TS cells were cultivated in self-renewing conditions (Stem Medium) or induced to differentiate for 4 days (Diff. Medium), in the absence or presence of Activin protein in the culture medium, mimicking Nodal stimulation. *4311* and *Gcm-1* are trophoblast differentiation markers, *Mash2* is a transient-amplifying marker, and *Eomes* is a stem-cell marker (see text for details). Values are given relative to *GAPDH* expression. Note how TS cells undergo precocious differentiation only in the absence of Ecto and in the presence of TGFβ stimulation (+Activin). Data of a representative experiment are presented as mean + SD of two replicates.

FIGURE 12

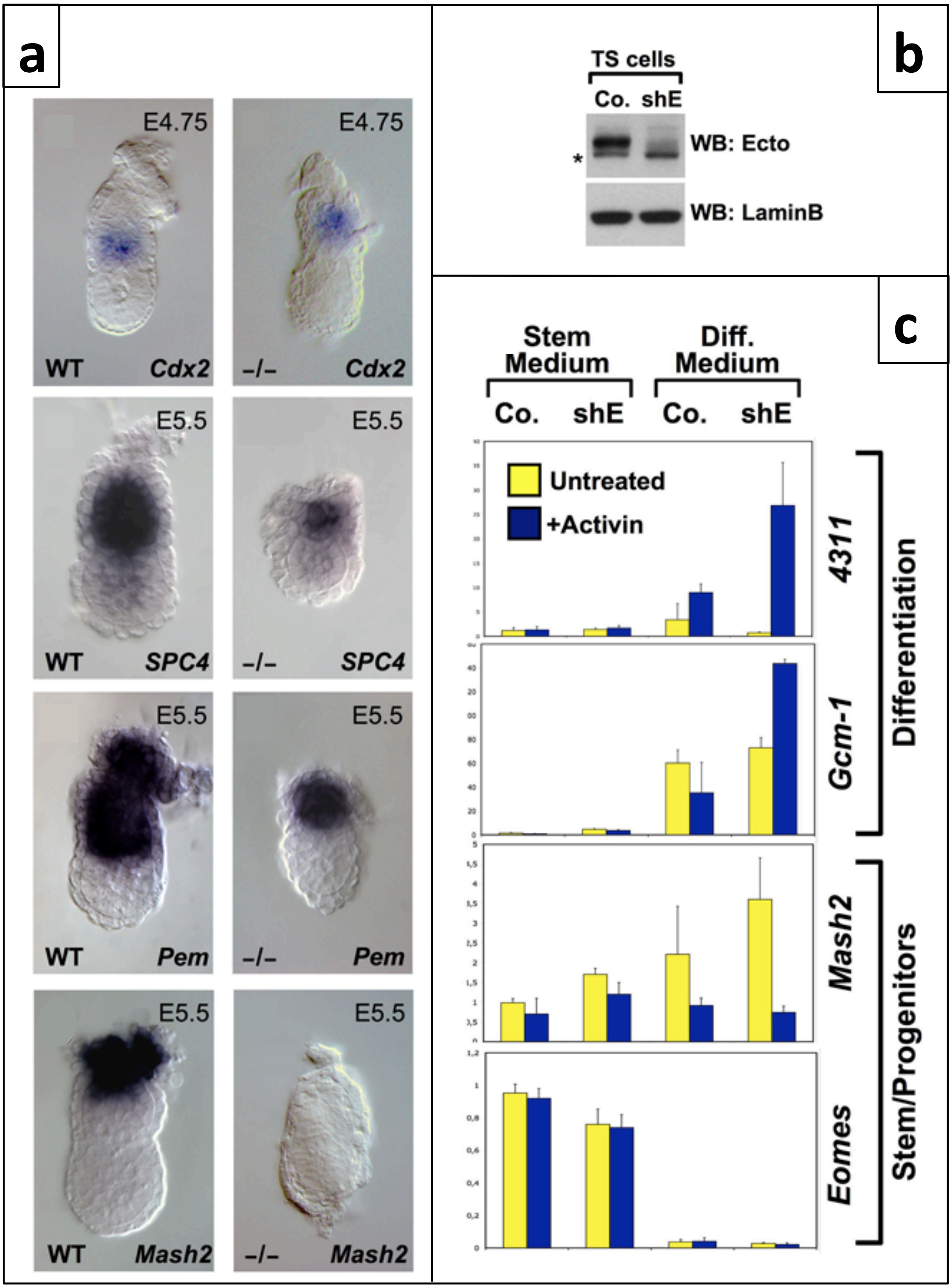
a
E4.75
WT
Cdx2
E4.75
–/–
Cdx2
E5.5
WT
SPC4
E5.5
–/–
SPC4
E5.5
WT
Pem
E5.5
–/–
Pem
E5.5
WT
Mash2
E5.5
–/–
Mash2
b
TS cells
Co.
shE
*
WB: Ecto
WB: LaminB
c
Stem Medium
Diff. Medium
Co.
shE
Co.
shE
Untreated
+Activin
4311
Gcm-1
Differentiation
Mash2
Eomes
Stem/Progenitors

Figure 13. *Ecto-/-* embryos allow exploring the HIGH SIGNALING part of the French flag for Nodal signaling in EXE.

a) Left, immunofluorescent stainings for the mitotic marker phospho-Histone3 (P-H3, red channel) on wild-type and *Ecto* mutant embryos at E5.0. YOYO1 serves as nuclear counterstain (green channel).

Right, quantitations of P-H3 positive cells in the embryonic (Em.) and extraembryonic (Ex.) portions of wild-type (n=17) and *Ecto* mutant (n=5) embryos. The number of P-H3 positive cells in each embryo was determined based on z-stack confocal images covering the whole embryo. Data are given as mean + SD.

b) A schematic model for the Nodal functions pertaining the trophoblast compartment. *Nodal-/-* embryos allow discovering the FGF4-mediated pro-stemness function of Nodal at E6.5. *Ecto* presence at earlier stages (around E5.5) is indispensable for further development of the trophoblast stem cells compartment: Ecto inhibits the strong pro-differentiative signal triggered by Nodal itself. Coherently, *Nodal-/-* embryos display trophoblast cells freezed in a transit-amplifying (i.e. Mash2 positive) state, because they lack this pro-differentiative Nodal effect.

c) Nodal acts as a morphogen for the trophoblast compartment: it triggers different responses in target cells at different dosage. In particular, low Nodal results in poor proliferation; normal Nodal allows wild type development; high Nodal ensues wholesale trophoblast differentiation.

FIGURE 13

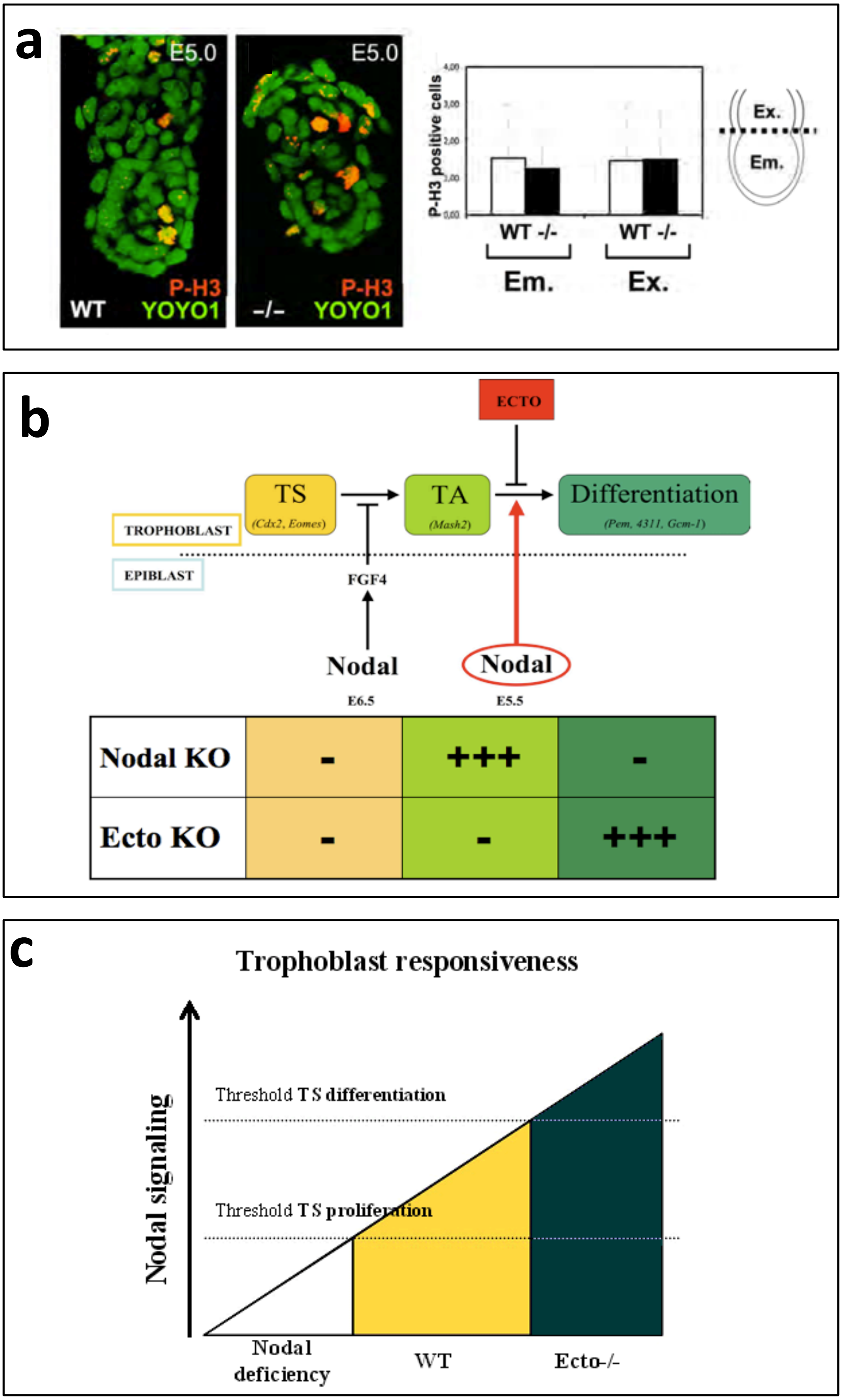
a
E5.0
E5.0
P-H3
WT
YOYO1
P-H3
-/-
YOYO1
P-H3 positive cells
4,00
3,00
2,00
1,00
0,00
WT -/-
WT -/-
Em.
Ex.
Ex.
Em.
b
ECTO
TS
(Cdx2, Eomes)
TA
(Mash2)
Differentiation
(Pem, 4311, Gcm-1)
TROPHOBLAST
EPIBLAST
FGF4
Nodal
E6.5
Nodal
E5.5
c
Trophoblast responsiveness
Nodal signaling
Threshold TS differentiation
Threshold TS proliferation
Nodal deficiency
WT
Ecto-/-

Nodal KO	-	+++	-
Ecto KO	-	-	+++

Figure 14. Lack of mesoderm in *Ecto* mutants is caused by excessive Nodal and defective EXE development.

First two rows: reduction of *Nodal* rescues mesoderm formation in *Ecto* mutant embryos, as assayed by *Eomes* expression and *T*. Lateral views, anterior to the left.

Third row: analysis of *Lim1* expression in AVE of wild-type (WT), *Ecto* mutants and *Ecto-/-; Nodal*+/- embryos.

Note how *Ecto-/-; Nodal*+/- embryos (red box) show already rescued mesoderm and EXE development (white arrowheads), but still display expanded AVE, suggesting that lack of mesoderm in *Ecto* mutants is primarily due to lack of EXE-derived inducing signal.

The table below shows how EXE and mesoderm markers are coupled throughout the mutants' series, whereas AVE seems uncoupled in *Ecto-/-; Nodal*+/- embryos. Tick marks stand for normal tissue; X marks stand for impaired tissue; arrows up stand for expanded tissue.

FIGURE 14

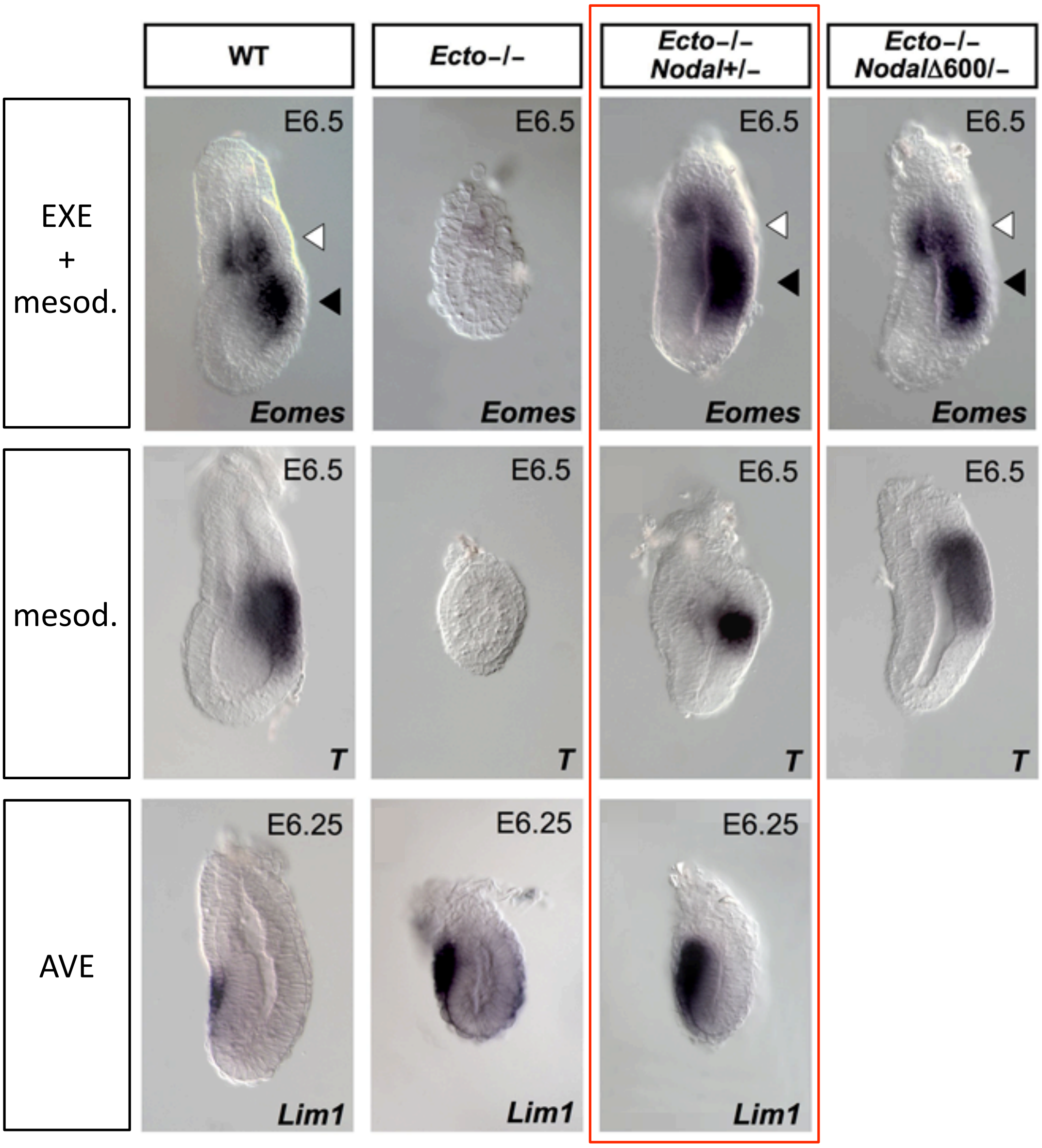
WT
Ecto–/–
Ecto–/–
Nodal+/–
Ecto–/–
NodalΔ600/–
EXE
+
mesod.
E6.5
Eomes
E6.5
Eomes
E6.5
Eomes
E6.5
Eomes
mesod.
E6.5
T
E6.5
T
E6.5
T
E6.5
T
AVE
E6.25
Lim1
E6.25
Lim1
E6.25
Lim1

EXE	✓	✗	✓	✓
mesod.	✓	✗	✓	✓
AVE	✓	↑↑	↑↑	✓

Figure 15. Massive Organizer induction in epiblast-specific *Ecto* mutants (*EpiKO*).

a) Immunofluorescent staining of wild-type (WT) and *Ecto*-/- (-/-) embryos with anti-Ecto antibody. Ecto is ubiquitously expressed, displaying a strong enrichment in epiblast cells at E5.5.

b) Immunoprecipitation of ubiquitinated-Smad4 from dissected Distal (D) and Proximal (P) portions of the embryonic cup at E7.0. Upper panel shows anti-Smad4 (Sm4) immunoblot of anti-Ubiquitin (Ub) immunoprecipitates. Co. is anti-Ubiquitin antibody alone. Lower panels show immunoblotting of embryonic whole extracts.

c) Expression of the anterior mesoderm marker *FoxA2* encompasses the whole primitive streak in *Sox2-Cre;Ecto fl/-* (*EpiKO*) streak stage embryos. Lateral and posterior views of a wild-type embryo (WT), and lateral and posterior views of an *EpiKO* embryo are provided. Dashed lines indicate the boundary between extraembryonic (EXE) and embryonic (epi.) tissues.

d) Expansion of the node in *EpiKO* embryos. Pictures show a close-up of the distal region of sibling embryos stained for the node marker *FoxA2*, taken from the anterior.

e) In situ hybridizations for the definitive endoderm marker *Cerl* at E7.5. Lateral views, anterior to the left. Below are shown transverse sections of the corresponding embryos, taken at the level of white lines.

f) *EpiKO* embryos display a widened and duplicated anterior node, as assayed by expression of *Shh* and *T* at E8.5/9.0. Pictures show a close-up of the node region, anterior to the top. Below are shown corresponding whole embryo lateral views. White arrowheads show the direction from which close-ups were taken.

FIGURE 15

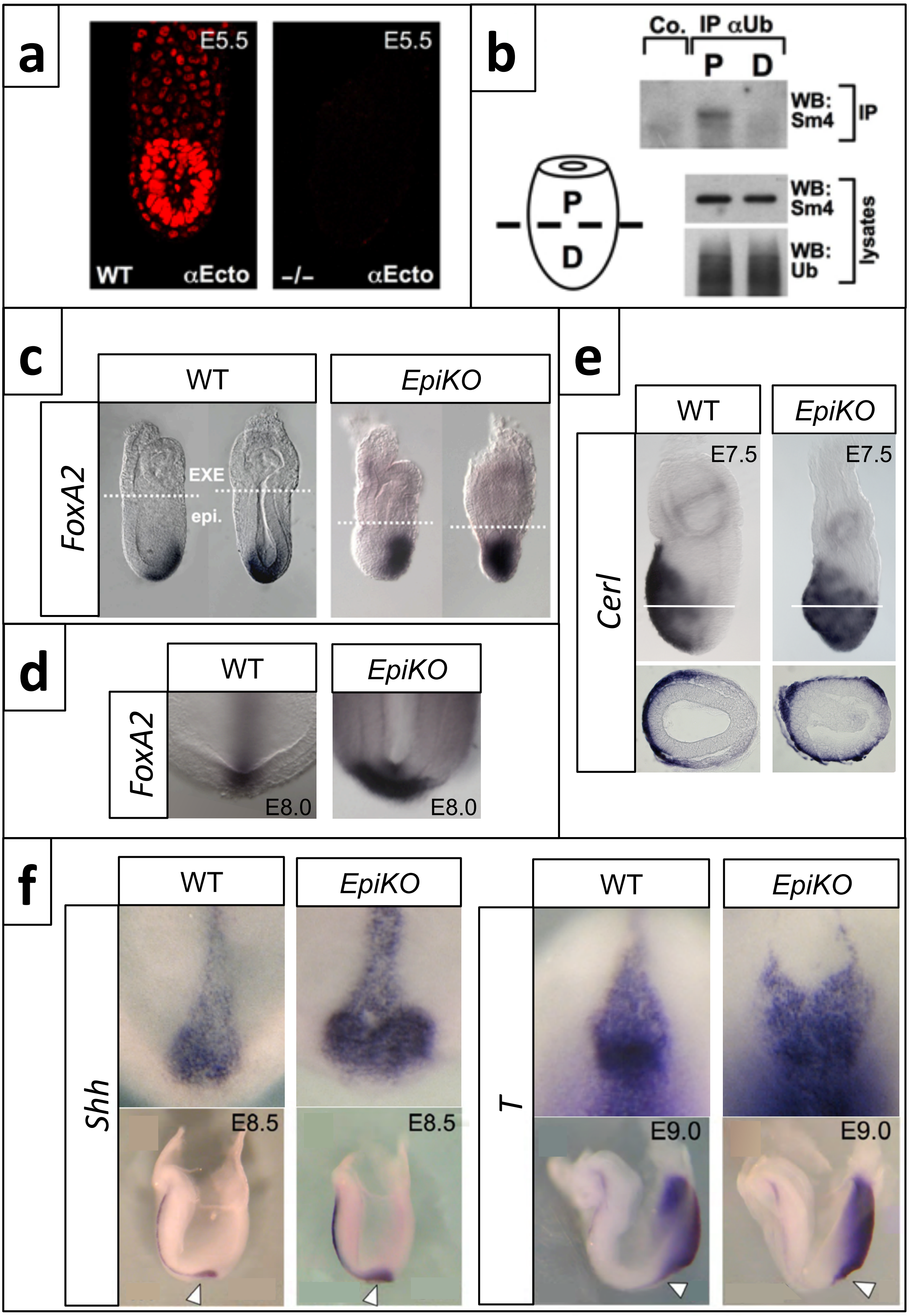
a
E5.5
WT
αEcto
E5.5
–/–
αEcto
b
Co.
IP αUb
P
D
WB: Sm4
IP
P
D
WB: Sm4
WB: Ub
lysates
c
WT
EpiKO
FoxA2
EXE
epi.
d
WT
EpiKO
FoxA2
E8.0
E8.0
e
WT
EpiKO
Cerl
E7.5
E7.5
f
WT
EpiKO
Shh
E8.5
E8.5
WT
EpiKO
T
E9.0
E9.0

Figure 16. Early Nodal related defects in epiblast specific *Ecto* knockout embryos, and schemes of the proposed model.

a) Left, *Ecto* inactivation from epiblast cells causes a precocious expression of *FoxA2* in the posterior proximal epiblast (arrowhead), at a stage when *FoxA2* is normally expressed only in AVE cells.

Right, *Sox2-Cre;Ecto fl/-* (*EpiKO*) embryos display enhanced and broadened *Nodal* expression at E6.5, likely reflecting unrestrained feed-forward Smad activity within the epiblast. On the contrary, *Nodal* is comparably expressed in wild-type and *EpiKO* embryos at E5.5.

b,c) When *Ecto* is selectively inactivated in epiblast cells, extraembryonic tissues development occurs normally, but unrestrained Smad4 activity, coupled to a feed-forward amplification of *Nodal* transcription, causes the complete anteriorization of the primitive streak (PS). This also suggests that in the absence of intracellular inhibition of Smad signaling by Ecto, extracellular cues secreted by the AVE and EXE are not sufficient to pattern the mesoderm. P: posterior PS fates. A: node/anterior PS fates. See discussion for details.

d) The Nodal morphogenetic field is shaped by differential responsiveness rather than by graded ligand availability. From right to left: a proximo-distal gradient of monoubiquitinated-Smad4 (Fig. 15b), results in a distal to proximal gradient of Smad4 activity that, coupled with an even ligand distribution, alone is able to shape a distal to proximal gradient of Nodal activity and to correctly pattern the primitive streak along its antero-posterior axis. See discussion for details.

FIGURE 16

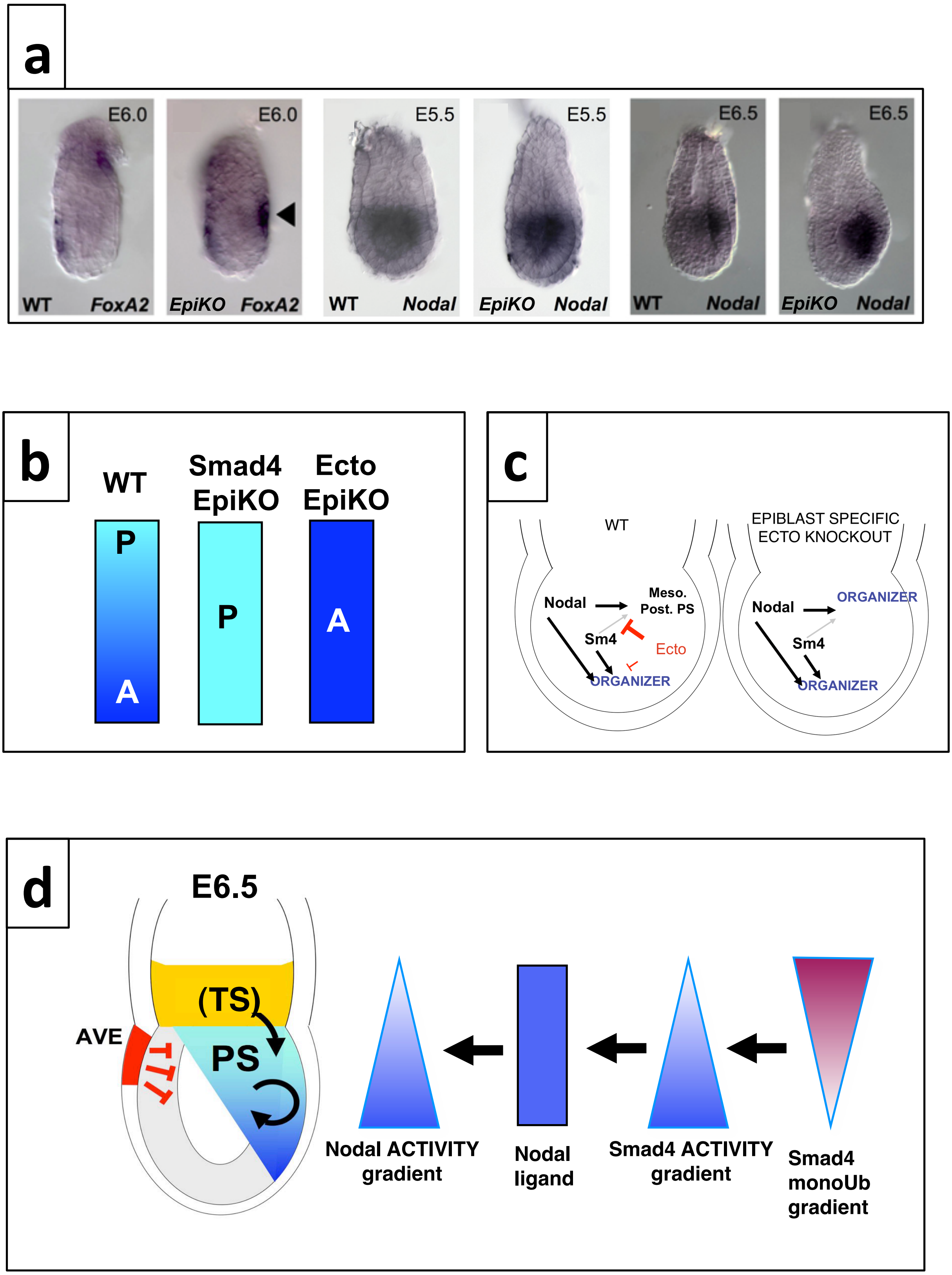
a
E6.0
WT
FoxA2
E6.0
EpiKO
FoxA2
E5.5
WT
Nodal
E5.5
EpiKO
Nodal
E6.5
WT
Nodal
E6.5
EpiKO
Nodal
b
WT
P
A
Smad4
EpiKO
P
Ecto
EpiKO
A
c
WT
Nodal
Meso.
Post. PS
Sm4
Ecto
ORGANIZER
EPIBLAST SPECIFIC
ECTO KNOCKOUT
Nodal
ORGANIZER
Sm4
ORGANIZER
d
E6.5
(TS)
AVE
PS
Nodal ACTIVITY
gradient
Nodal
ligand
Smad4 ACTIVITY
gradient
Smad4
monoUb
gradient

Supplemental Table 1

PCR oligonucleotides used for genotyping of mouse offspring and embryos. The expected length of the amplified fragment is indicated on the right-most column (BAND) for each allele.

SUPPLEMENTAL TABLE 1

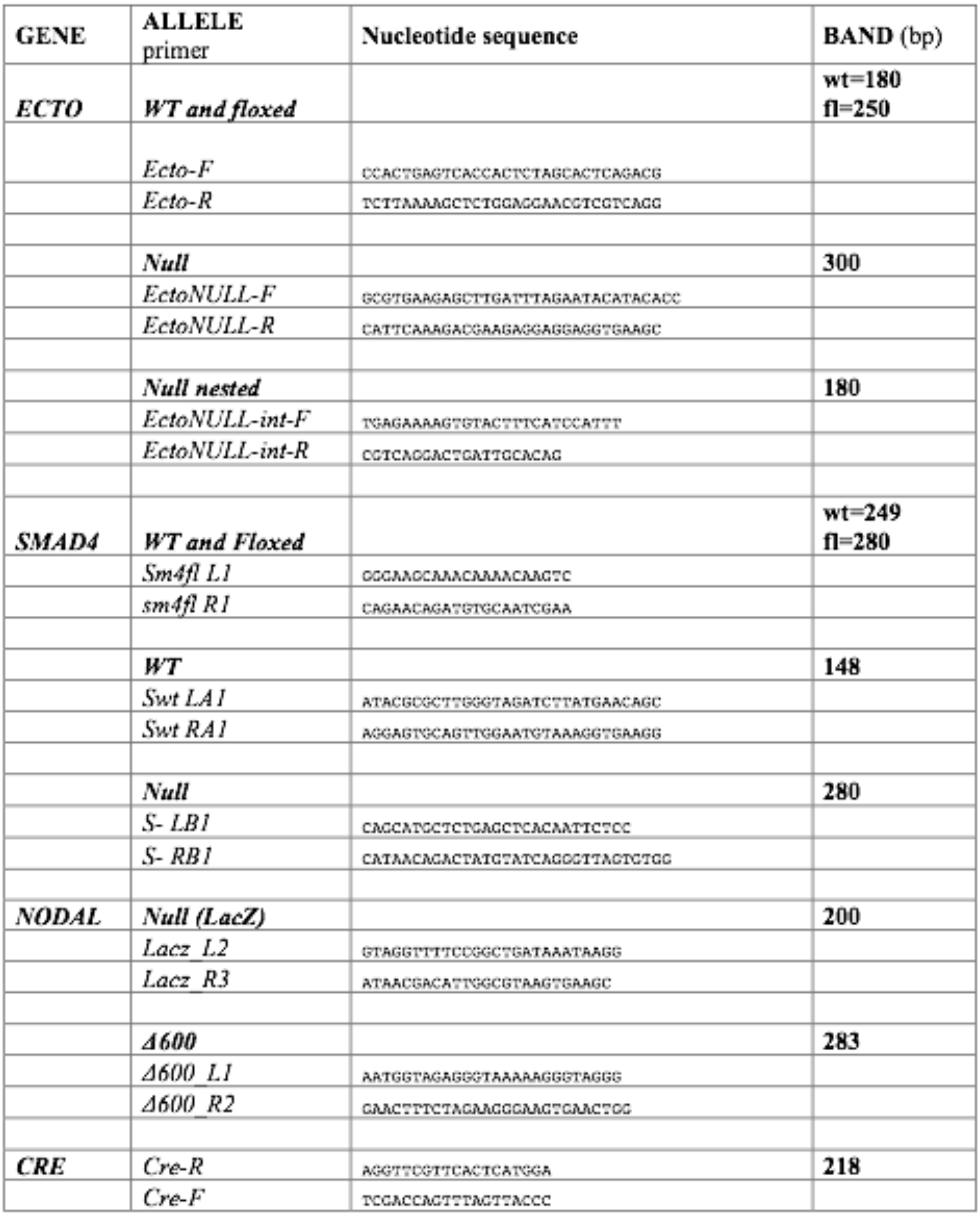

GENE	**ALLELE** primer	**Nucleotide sequence**	**BAND** (bp)
ECTO	***WT and floxed***		**wt=180** **fl=250**
	Ecto-F	CCACTGAGTCACCACTCTAGCACTCAGACG	
	Ecto-R	TCTTAAAAGCTCTGGAGGAACGTCGTCAGG	
	Null		**300**
	EctoNULL-F	GCGTGAAGAGCTTGATTTAGAATACATACACC	
	EctoNULL-R	CATTCAAAGACGAAGAGGAGGAGGTGAAGC	
	Null nested		**180**
	EctoNULL-int-F	TGAGAAAAGTGTACTTTCATCCATTT	
	EctoNULL-int-R	CGTCAGGACTGATTGCACAG	
SMAD4	***WT and Floxed***		**wt=249** **fl=280**
	Sm4fl L1	GGGAAGCAAACAAAACAAGTC	
	sm4fl R1	CAGAACAGATGTGCAATCGAA	
	WT		**148**
	Swt LA1	ATACGCGCTTGGGTAGATCTTATGAACAGC	
	Swt RA1	AGGAGTGCAGTTGGAATGTAAAGGTGAAGG	
	Null		**280**
	S- LB1	CAGCATGCTCTGAGCTCACAATTCTCC	
	S- RB1	CATAACAGACTATGTATCAGGGTTAGTGTGG	
NODAL	***Null (LacZ)***		**200**
	Lacz_L2	GTAGGTTTTCCGGCTGATAAATAAGG	
	Lacz_R3	ATAACGACATTGGCGTAAGTGAAGC	
	Δ600		**283**
	Δ600_L1	AATGGTAGAGGGTAAAAAGGGTAGGG	
	Δ600_R2	GAACTTTCTAGAAGGGAAGTGAACTGG	
CRE	*Cre-R*	AGGTTCGTTCACTCATGGA	**218**
	Cre-F	TCGACCAGTTTAGTTACCC	

Supplemental Table 2

PCR oligonucleotides used for real-time analysis of TS cell differentiation.

SUPPLEMENTAL TABLE 2

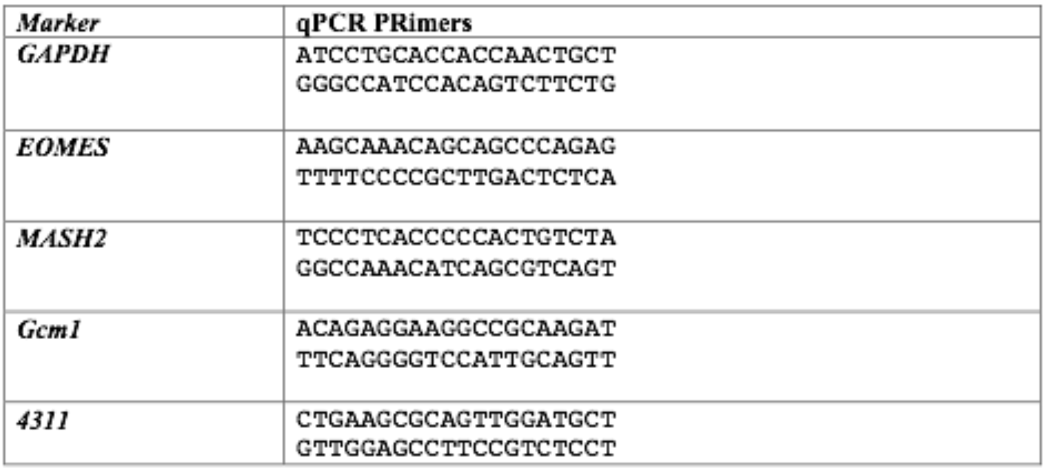

Marker	**qPCR PRimers**
GAPDH	ATCCTGCACCACCAACTGCT GGGCCATCCACAGTCTTCTG
EOMES	AAGCAAACAGCAGCCCAGAG TTTTCCCCGCTTGACTCTCA
MASH2	TCCCTCACCCCCACTGTCTA GGCCAAACATCAGCGTCAGT
Gcm1	ACAGAGGAAGGCCGCAAGAT TTCAGGGGTCCATTGCAGTT
4311	CTGAAGCGCAGTTGGATGCT GTTGGAGCCTTCCGTCTCCT

ACKNOWLEDGMENTS

Firstly, I would like to thank Prof. Stefano Piccolo for giving me an opportunity to work in his lab, for his supervision and tremendous support over the past three years. I specifically thank Sirio Dupont for his constant guidance, encouragement, discussions and suggestions in day-to-day life in the lab. Many thanks go out to all those people who helped me a lot in the lab during these years; these people include Elena Enzo, Luca Zacchigna, Mariaceleste Aragona, Sandra Soligo Graziano Martello, Masafumi Inui, Marco Montagner, Maddalena Adorno, Michelangelo Cordonensi, Ananth Mamidi, Andrea Manfrin, Francesca Zanconato, Luca Schiesari. I wish also to thank Professor Argenton and Professor Bressan for transferring to me some parts of their experience.

To my friends, thanks for having walked and keep walking along with me in good and bad times. To my family, thanks for your love and support. To my wife, thanks for everything.